Available online at www.sciencedirect.com
ScienceDirect
Journal of Chromatography A, 1149 (2007) 254–273
JOURNAL OF CHROMATOGRAPHY A
www.elsevier.com/locate/chroma

Viscous fingering in packed chromatographic columns: Linear stability analysis

G. Rousseaux [a,1], A. De Wit [a], M. Martin [b,*]

[a] *Nonlinear Physical Chemistry Unit and Center for Nonlinear Phenomena and Complex Systems, Université Libre de Bruxelles (U.L.B.), CP 231, 1050 Brussels, Belgium*
[b] *Ecole Supérieure de Physique et de Chimie Industrielles, Laboratoire de Physique et Mécanique des Milieux Hétérogènes (PMMH, UMR 7636 CNRS, ESPCI, Université Paris 6, Université Paris 7), 10 rue Vauquelin, 75231 Paris Cedex 05, France*

Received 22 December 2006; received in revised form 6 March 2007; accepted 13 March 2007
Available online 19 March 2007

Abstract

When a fluid is displaced by a less viscous one in a porous medium, a hydrodynamic instability appears leading to the formation of some kind of fingers of the upstream fluid invading the downstream one, hence the name "viscous fingering" (VF) given to this instability. In a LC column, such an instability is likely to appear at that of the two interfaces between the sample and the eluent which exhibits an unfavorable viscosity contrast. It leads to distorted peak shapes and contributes to peak broadening. This phenomenon has been observed for long in SEC and more recently in RPLC on elution peak shapes as well as with various methods of in-column visualization. A simplistic LC column model is described to explain the origin of the VF instability and its characteristics. The general principles for analyzing hydrodynamic instabilities are described and the results of the linear stability analysis performed by Tan and Homsy [C.T. Tan, G.M. Homsy, Phys. Fluids 29 (1986) 3549 [1]], at the onset of the VF phenomenon for a step interface between two fluids are here applied to typical operating conditions encountered in analytical LC. The most probable growth rate and wavelength (linked to the finger width) of the instability are given in terms of particle size and solute diffusion coefficient, with particular emphasis on the role of the carrier velocity. Previously published qualitative observations about VF in chromatography are examined and interpreted at the light of this theory. The role of the column geometry on the development of the instability, the possible sources of noise or fluctuations triggering the instability, and the various experimental situations in which a significant viscosity contrast is encountered in LC are discussed.

Keywords: Viscous fingering; Linear stability analysis; Porous media; Liquid chromatography; Sample viscosity; Hydrodynamic instability

1. Introduction

According to the Giddings' classification of separation methods, chromatography, as well as field-flow fractionation, belong to the F(+) group. In methods of this group, the slight enrichment of one component with respect to the other sample components in the direction of the chemical potential gradient created by a field or an interface is considerably amplified by the flow of a carrier fluid in a direction essentially perpendicular to that of the chemical potential gradient [2]. The flow does not contribute to the separation selectivity by itself. However, because it allows the slight enrichment step to be repeated many times in a cascade-like manner, the carrier flow is an essential ingredient of the separation process. The characteristics of this carrier flow have thus a profound impact on the efficiency of the separation.

Generally, separation scientists and chromatographers consider the flow of carrier fluid as being basically stable, i.e. without irregularities in time and in space (except for axial velocity variations arising from fluid compressibility in gas and supercritical fluid chromatography, and, to a lesser extent, in ultra-high pressure liquid chromatography). Most often, they even do not suspect that the flow may not be stable. Still, nearly all modern studies in fluid mechanics are dealing with investigations of flow instabilities arising in many situations, under certain conditions. It is thus of utmost importance to understand the process of development of the instabilities, to specify under which experimental conditions the flow of carrier fluid in the separation

* Corresponding author. Tel.: +33 1 4079 4707; fax: +33 1 4079 4523.
E-mail address: martin@pmmh.espci.fr (Michel Martin).
[1] Present address: Université de Nice-Sophia Antipolis, INLN UMR 6618 CNRS-UNICE, 1361 route des Lucioles, 06560 Valbonne, France.

0021-9673/$ – see front matter © 2007 Elsevier B.V. All rights reserved.
doi:10.1016/j.chroma.2007.03.056

conduit can be stable, and to be able to evaluate quantitatively the influence of the instabilities on the separation performances. Indeed, if this flow is unstable, it is likely to be detrimental to the separation efficiency (Giddings then spoke of "parasitic flow" [2]).

One potential source of concern for the development of flow instabilities in chromatography arises from the fact that the fluids displaced in the chromatographic system have generally different viscosities. This is true when a liquid chromatographic run is performed under gradient elution conditions since the viscosity of the carrier mixture is a function of its composition [3]. But even in isocratic conditions, the viscosity of the sample injected in the column is most often different from that of the carrier liquid. The difference in viscosity between two fluids (the carrier liquid and the sample) may be the source of a viscous fingering instability. Indeed, viscous fingering occurs as soon as one fluid displaces another more viscous one inside a porous medium. The initially planar interface starts then to deform as "fingers" of one fluid invading the other one, hence the word "fingering" used to describe the phenomenon.

That the interface between two liquids may be deformed when they flow through a porous medium was first noticed by Hill who observed a phenomenon that he called "channelling" during the displacement of sugar solutions by water in a packed column [4]. The stability of the interface between two non-miscible fluids was later studied by Saffman and Taylor [5] and the viscous fingering instability between immiscible liquids is frequently called today the "Saffman–Taylor instability", although the phenomenon should have been called the "Hill instability" from a historical perspective according to Homsy [6]. Saffman and Taylor investigated the shapes and dynamics of the fingers obtained in a so-called Hele–Shaw cell, after the system devised by this author [7], i.e. the channel obtained between two fixed parallel plates separated by a small distance [8]. Indeed, it can be shown that the motion in a Hele–Shaw cell is mathematically analogous to the two-dimensional flow in a porous medium [5,9a].

The viscous fingering instability typically occurs when water displaces petroleum in underground reservoirs which explains why experimental and theoretical studies on viscous fingering have appeared mainly in the petroleum engineering and physics literature [6]. Still, in chromatography, the first experimental evidence of the perturbations on the peak characteristics (modified retention time, increased band broadening and distorted peak shape) arising from a high sample viscosity is found in the work of Flodin on the desalting of proteins by means of the gel filtration version of size exclusion chromatography (SEC) [10]. While later SEC studies reported perturbations due to sample concentration effects, Flodin clearly noticed that "the viscosity of the sample rather than the concentration is the limiting factor". Still, the origin of the perturbations was believed to arise in part from the enhanced compression of the relatively soft bed used at that time in gel filtration chromatography while the viscous sample zone traveled along the column. The first mention of viscous fingering (VF) in chromatography is found in a chapter by Altgelt and Moore [11]. They wrote that "the more abrupt the viscosity change at the rear boundary of the sample zone, the less stable that boundary becomes" and that "the extra pressure drop caused by sample viscosity then permits the solvent to push through at some weak point, and the liquid velocity profile becomes very uneven until considerable spreadout has occurred" after some studies of fluid flow in packed beds. Although these studies were then not referenced, Moore later made reference to Collins' book [12] in connection to the fact that "the pattern of erratic delay (of the chromatographic peaks) is indicative of viscous fingering" [13]. Clearly, the phenomenon is attributed to flow effects rather than to packing effects. In spite of the fact that, in the early 70's, it is reported that "considerable qualitative discussion has taken place in recent years concerning the so-called viscous fingering effect" in SEC [14], only a few brief mentions of VF are found in the chromatographic literature of that period, with, at best, a reproduction of the description found in the above-mentioned chapter by Altgelt and Moore [14–18]. Besides, several studies showed the influence of the polymer sample viscosity or concentration in SEC on retention and peak shape that can be attributed to VF [19–22]. In the late 70s and in the 80s, various studies were performed on the influence of the polymer sample concentration on the mean elution volume in SEC columns [23–27]. They further illustrated that the variations of retention and the distortion of the peak shapes arising from the viscosity effect occur in the interstitial volume of the porous bed and confirmed that the significant factor controlling the phenomenon is the relative viscosity difference between the sample solution and the eluent. However, they showed, as already noticed earlier [14], that VF cannot be wholly responsible for the change in elution volume and that other effects, like concentration-induced change in macromolecular dimensions, are simultaneously occurring in SEC of polymers. Still, contradictory conclusions were derived about the relative importance of the various concentration effects [28,29]. Nevertheless, a rough guide was that the sample viscosity should not be greater than twice that of the carrier liquid, both in classical fixed cylindrical packed columns [30a,31] and in annular rotating chromatographic beds [32].

In all experiments described above, except those of Flodin, the chromatographic peaks which were distorted because of the VF phenomenon were those of substances which were directly causing the enhancement of the sample viscosity well above that of the eluent. They were in these cases macromolecular substances present at a relatively large concentration in the sample. In Flodin experiments [10], the sample viscosity was controlled by means of the concentration of dextran while the distorted peaks were those of other sample substances (haemoglobin or sodium chloride) present at relatively low concentrations. Similarly, Czok et al. [33] performed SEC experiments in which the viscosities of either the protein sample or the aqueous carrier or both were modified by means of various concentrations of glycerol. Peak distortion appeared on the tailing edge when the sample was more viscous than the carrier, and on the leading edge in the opposite case. In the former case, they could limit the distortion by injecting a plug of viscous eluent immediately following sample injection. For the first time, they noticed that the distorded peak shapes were not reproducible. Comparable experiments were later performed by Cherrak et al. [34] who also

observed the irreproducibility of the toluene peak shapes when the carrier liquid and the sample solvent had different concentrations of isopropanol in methanol. They noticed a significant loss of efficiency when the eluent and sample viscosity differed by more than 10%. Peak distortions of either unretained or retained analytes arising from the viscosity difference between sample and eluent have also been observed and investigated in reversed-phase liquid chromatography with water–acetonitrile or water–alcohol (isopropanol or methanol) mixtures by Castells and coworkers [35–37]. Again, the position of the peak maxima and shoulders appeared irreproducible.

Further evidence of fingering in chromatographic columns is provided by visualization experiments. Altgelt noticed he observed fingering arising from steep density gradients by means of colored samples [38]. Examining the shapes of protein zones by slicing frozen gel beds, Yamamoto et al. [27] found a wide spreading of the sample zone in the radial and longitudinal directions. Visualization, by NMR imaging, of solutions containing a gadolinium complex or of proteins chelating the gadolinium ion inside the porous medium allowed to follow the dynamics of viscous fingers along a SEC column and their three-dimensional structure [39,40]. Interestingly, in spite of the limited resolution of the imaging system, Plante et al. [39] observed some finger formation near the column inlet for moderate protein concentrations while the chromatographic peak recorded at the column outlet has a symmetrical Gaussian-like shape which does not allow to suspect that some perturbations occurred inside the column. Still such perturbations necessarily have contributed to enhance the peak broadening. This additional band broadening can be falsely attributed to another zone dispersion mechanism and erroneous conclusions can be derived about the latter. Peak distortion appear on the tailing edge at larger sample concentrations. This NMR imaging technique was used to investigate the effects of the permeability heterogeneity on VF [41], and to design flow distributors and column configurations for reducing this perturbing phenomena [42,43]. Using an alternative NMR imaging technique, the simultaneous visualization of the effect of VF on the migration of several, differently retained, sample components was rendered possible [44].

Recently, by matching the refractive indices of the mobile phase, the stationary phase and the bed container, Broyles et al. [45] developed an optical method allowing to visualize, with the eye or a photographic detector, the migration of a colored sample component in a chromatographic column. In particular, this approach was used to visualize the development of viscous fingers with a resolution that appears superior to that of the NMR images. The influence of the column header design was investigated by this method [46], as well as the onset of VF in the chromatographic column [47]. The effect of VF arising from the change of carrier liquids (made of methanol/water or acetonitrile/water mixtures of various compositions) in multidimensional reversed-phase liquid chromatography on analyte peak shapes was emulated by injecting analytes dissolved in the first dimension carrier into the chromatographic system of the second dimension [48].

In spite of the number of articles cited above, the chromatographic community is largely unaware of the VF phenomenon and of its potentially harmful effects for the separation performances. Furthermore, apart from an expression of the fastest growing finger wavelength found in papers by Fernandez and coworkers [39,42,44,49], all other descriptions of VF in chromatography are essentially qualitative or phenomenological and do not contain any theoretical background of the phenomenon. In this context, it is the objective of this article to discuss the properties of VF in chromatographic columns from a theoretical perspective, to analyze in which conditions this instability is to be expected, and what will then its characteristics be. Using the linear stability approach developed by Tan and Homsy [1], we show how a simple model of viscous fingering between two miscible fluids of different viscosities can provide information on the typical length and time scales of the fingering pattern appearing at the onset of the instability. While the results of such a linear stability analysis are frequently presented in the fluid mechanics literature by means of dimensionless quantities, we extend them and show how they rely on relevant chromatographic quantities, such as carrier velocity, particle size and solute diffusion coefficient. A discussion of experimental results available in chromatography in terms of our theoretical predictions is also provided.

The outline of the article is therefore organized as follows: Section 2 will first recall the physical mechanisms and important parameters related to the hydrodynamic fingering instability. Section 3 will introduce the theoretical model to be used to describe the fingering properties, recall the principles of a linear stability analysis (LSA) and discuss the dispersion relation curves. Explanations on physical informations that can be obtained from such a LSA will be given in that section as well. Concrete applications to the case of chromatographic columns will be discussed in Section 4 with particular emphasis on the role of the carrier velocity. In Section 5, the effect of the evolution of the profile of the interface on the characteristics of the VF pattern, the role of the column geometry, the origin of the noise triggering the instability are discussed. Previously published qualitative observations about VF in chromatography are examined and interpreted at the light of this theory, and the various experimental situations in which a significant viscosity contrast is encountered in LC are discussed in Section 5 before conclusions are drawn in Section 6.

2. Physical mechanism of viscous fingering

To understand the origin of the viscous fingering phenomenon in porous media, we present below a simple model making use of flow equations classically used in packed column chromatography. To give more generality to the derived conclusions, we also consider the hydrostatic pressure contribution to flow. Although this contribution to the mean flow velocity is usually negligible in modern liquid chromatography, it has to be discussed in which conditions its contribution to the hydrodynamic instabilities, which gives rise to the density fingering phenomenon already observed in early SEC experiments [38], is negligible compared to that leading to viscous fingering.

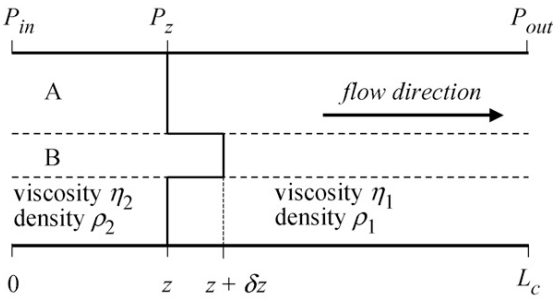

Fig. 1. Schematic illustration of a perturbation of the interface between two fluids in a packed column, pushing the upstream liquid 2 in a small part (B) of the column cross-section ahead of the position of the interface in the main part (A) of the cross-section.

2.1. Simple model of flow instability

Let us consider a packed column of length L_c initially filled with a liquid 1 of viscosity η_1. A constant pressure pump is delivering a liquid 2 of viscosity η_2, which is displacing the downstream fluid 1. Let ΔP be the constant pressure drop applied along the column. When the hydrostatic contribution to the pressure drop is included, the basic flow equation for a porous medium containing a single fluid of viscosity η and density ρ is then expressed as, [50]:

$$u = \frac{k_p}{\eta}\left(-\frac{dP}{dz} + \rho\delta g\right) = \frac{k_p}{\eta}\left(\frac{P_{in} - P_{out}}{L_c} + \rho\delta g\right) \quad (1)$$

where P_{in} and P_{out} are the inlet and outlet applied pressures, respectively, k_p the column permeability (assumed to be constant throughout the whole column), g the gravitational acceleration and δ an indicator for the flow orientation equal to +1 for downward vertical flow, −1 for upward vertical flow, 0 for a horizontal column, and taking intermediate values for tilted columns. Obviously, for a horizontal column, there is no hydrostatic pressure and only VF instabilities can appear in the column. The latter equality in Eq. (1) assumes that the fluid is incompressible.

Let us now assume that, when the interface between the two fluids is at position z along the column, a perturbation is displacing the interface ahead of (or behind) that position in a small part (B) of the column cross-section. This perturbation is schematically represented in Fig. 1, the interface is at position $z+\delta z$ in the perturbed section B, and at position z in the main, unperturbed section A. For each section (A and B), considering the liquids as incompressible, the velocity of liquid 1 is the same as that of liquid 2, but the flow velocity, u_A, in section A is different from that, u_B, in section B. In this simple flow model, let us furthermore assume that there is no momentum exchange between sections A and B, hence that the flow velocity in section B is independent of that in section A.

When a fluid 2 is displacing a fluid 1 in the porous bed, a flow instability may arise from the viscosity difference, but also from the density difference when the upper fluid is denser than the lower fluid. The hydrodynamic instability arising from an unfavorable density gradient between two immiscible fluids is called the Rayleigh–Taylor instability. To derive the stability criterion when both viscosity and density instabilities come in interplay, let apply Eq. (1) for the two fluids in part A of the column cross-section shown in Fig. 1:

$$u_A = \frac{k_p}{\eta_2}\left(\frac{P_{in} - P_z}{z} + \rho_2\delta g\right) = \frac{k_p}{\eta_1}\left(\frac{P_z - P_{out}}{L_c - z} + \rho_1\delta g\right) \quad (2)$$

from which one gets, noting that $\Delta P = P_{in} - P_{out} = (P_{in} - P_z) + (P_z - P_{out})$:

$$\frac{\Delta P}{L_c} + \delta g\left[\rho_2\frac{z}{L_c} + \rho_1\left(1 - \frac{z}{L_c}\right)\right] = \frac{u_A}{k_p}\left[\eta_2\frac{z}{L_c} + \eta_1\left(1 - \frac{z}{L_c}\right)\right] \quad (3)$$

For the perturbed section B of the column cross-section, one gets, by replacing u_A by u_B and z by $z+\delta z$ in Eq. (2):

$$u_B = \frac{k_p}{\eta_1}\left[\frac{P_{z+\delta z} - P_{out}}{L_c - (z+\delta z)} + \rho_1\delta g\right] = \frac{k_p}{\eta_2}\left(\frac{P_{in} - P_{z+\delta z}}{z+\delta z} + \rho_2\delta g\right) \quad (4)$$

from which one gets:

$$\frac{\Delta P}{L_c} + \delta g\left[\rho_2\frac{z}{L_c} + \rho_1\left(1 - \frac{z}{L_c}\right)\right] = \frac{u_B}{k_p}\left[\eta_2\frac{z}{L_c} + \eta_1\left(1 - \frac{z}{L_c}\right)\right] + \frac{\delta z}{L_c}\left[\frac{u_B}{k_p}(\eta_2 - \eta_1) - \delta g(\rho_2 - \rho_1)\right] \quad (5)$$

Comparing Eqs. (3) and (5), one gets:

$$u_A - u_B = \frac{k_p}{[\eta_2(z/L_c) + \eta_1(1 - (z/L_c))]} \times \left[\frac{u_B}{k_p}(\eta_2 - \eta_1) - \delta g(\rho_2 - \rho_1)\right]\frac{\delta z}{L_c} \quad (6)$$

The denominator of the RHS member of this equation is positive. Hence, whether u_A is larger than u_B or not depends on the sign of the product of δz and of the term in brackets in the numerator of the RHS member of Eq. (6).

2.2. Stability criterion

Looking at Fig. 1 shows that the flow is stable when $u_A > u_B$ for $\delta z > 0$, and when $u_B > u_A$ for $\delta z < 0$. Hence, from Eq. (6), for both $\delta z > 0$ and $\delta z < 0$, the criterion of stability is expressed as:

$$\frac{u}{k_p}(\eta_2 - \eta_1) - \delta g(\rho_2 - \rho_1) > 0 \quad (7)$$

Since the velocity u_B marginally differs from the average flow velocity, u, the latter is used in this expression. It contains two terms, the first one represents the viscosity effect and the second one the density effect.

Let consider the situation where the former is dominating, for instance in horizontal flow ($\delta = 0$) or for isopycnic fluids ($\rho_1 = \rho_2$). From Eq. (7), the stability criterion becomes:

$$\eta_2 > \eta_1 \tag{8}$$

Let δz be positive, as shown in Fig. 1. When the criterion (8) is satisfied, $u_A > u_B$ and the perturbation is moving more slowly than the liquids in the main part of the column cross-section. The perturbation velocity decreases up to the point where the position of the interface in the main section A is catching that in the perturbed section, hence restoring the unperturbed state. This is well a stable situation. If, instead, $\eta_2 < \eta_1$, according to Eq. (6), $u_B > u_A$. In this case, the perturbation is moving faster than the main flow. It becomes amplified and the distance δz is increasing. The liquid 2 is protruding through the interface between liquids 1 and 2, forming some kind of finger, hence the name viscous fingering given to this hydrodynamic instability.

Let now δz be negative, i.e. the perturbation has acted in such a way that the interface in section B is lagging behind the main part of the interface. Then, if $\eta_2 > \eta_1$, according to Eq. (6), $u_B > u_A$, the interface in the perturbed section is moving faster than the main interface. The perturbation is decreasing again until the interface reaches the same position in the two sections. If now, $\eta_2 < \eta_1$, then, $u_B < u_A$. The interface in the perturbed section is lagging more and more behind the main interface. This is again an unstable situation.

This discussion illustrates that, when the viscosity term dominates the density term in Eq. (6), a perturbation of the interface is becoming amplified whenever $\eta_2 < \eta_1$. Hence, for a horizontal column, an interface is unstable when the displacing fluid is less viscous than the displaced fluid. Although some assumptions have been made to derive in a simple way Eqs. (1)–(6) which illustrate the behavior of a perturbation to the flow system, this above conclusion is valid when the system generating the pressure-driven flow is operated in constant flow as well as constant pressure conditions, and whether the fluids are incompressible or not.

When the second term of inequality (7) is dominating, for instance for isoviscous fluids, the stability criterion becomes:

$$\delta(\rho_2 - \rho_1) < 0 \tag{9}$$

which, whatever the flow orientation, expresses that the flow is stable when the lower fluid is the denser. If the reverse is true, then the heavier fluid lies above the lighter one in the gravity field and a Rayleigh–Taylor instability is observed.

When the viscosity and density effects are both present, various situations can be encountered. The flow is always stable when the displacing fluid is more viscous than the displaced one ($\eta_2 > \eta_1$) and when the lower fluid is the denser ($\delta(\rho_2 - \rho_1) < 0$, i.e. $\rho_1 > \rho_2$ for downward flow and $\rho_2 > \rho_1$ for upward flow). Conversely, the flow is always unstable when the displacing liquid is the less viscous one and when the upper fluid is the denser one. In the other situations, whether the flow is stable or not depends on the flow velocity u. When $\eta_2 > \eta_1$ (i.e. when the viscous contrast itself leads to a stable flow), inequality (7) shows that the flow is stable if the viscous term overcomes the gravitational term, i.e. if u is larger than a critical velocity u_c expressed by:

$$u_c = k_p g \left| \frac{\rho_2 - \rho_1}{\eta_2 - \eta_1} \right| \tag{10}$$

If, instead, $\eta_2 < \eta_1$, inequality (7) shows that the flow is stable if u is smaller than u_c, i.e. if the stabilizing density difference term overcomes the destabilizing viscosity difference term. The above stability criterion was first obtained by Hill [4], then by several authors by means of various arguments [5,6,9b,12,51–53].

The stability criterion expressed by inequality (7) can be written as:

$$\Delta P_{app} \frac{\Delta\eta}{\eta} - \delta \Delta P_{stat} \frac{\Delta\rho}{\rho} > 0 \tag{11}$$

where ΔP_{app} is the applied pressure drop and ΔP_{stat} the hydrostatic pressure when the column contains liquid 1, and $\Delta\eta/\eta$ and $\Delta\rho/\rho$ are the relative viscosity and density differences between liquids 2 and 1, respectively. In liquid chromatography (LC), the applied pressure drop is generally of the order of 100 bars or more and the hydrostatic pressure for a vertical column of the order of 0.01 bar (for water, the hydrostatic pressure for a 10 m long column is about 1 bar). In order for the density term to be comparable to the viscosity term in relation (11), the relative density difference should therefore be 10^4 times larger than the relative viscosity difference. In practice, the relative density difference rarely exceeds 1 and is frequently of the order 0.2 or less. The influence of the density effect in the flow stability should therefore be similar to that of the viscosity effect for a relative viscosity difference of 10^{-4} or less. Experiments on fronts as well as numerical simulations and linear stability analysis show that such a relative viscosity change is much too small to observe a significant fingering effect during the transit time across a typical column. Therefore, it appears that, in modern LC, the influence of the density difference on the flow stability in vertical columns is negligible compared to that of the viscosity effect, at least at the onset of the instability. Therefore, only viscous fingering will be further analyzed in this article.

2.3. Case of miscible fluids

In the above discussion about the stability criterion for viscous fingering, it has not been specified whether the fluids are miscible or not. In situations of interest in liquid chromatography, liquids 1 and 2 are most often miscible. Then, a refined analysis for miscible liquids shows that, if c is the concentration of downstream liquid 1 in the binary mixture, which can be set to vary from 0 for liquid 2 to 1 for liquid 1 without lost of generality, the stability criterion becomes [54,55]:

$$\left.\frac{d\eta}{dc}\right|_{c=0} + \left.\frac{d\eta}{dc}\right|_{c=1} < 0 \tag{12}$$

This criterion depends on the variation of the viscosity, η, of the mixture with c. When the viscosity of the mixture decreases monotonically with the increasing concentration c of fluid 1 in fluid 2, at the two end-points of the viscosity–concentration curve, the derivatives of the viscosity with respect to the

concentration are negative and condition (12) is satisfied. Conversely, the flow is unstable when the viscosity increases steadily with increasing c. Thus, for fluids with monotonic viscosity–concentration curves, the stability criterion expressed by relation (12) is identical to that given by relation (8).

When the viscosity–concentration curve is not monotonic, $d\eta/dc|_{c=0}$ and $d\eta/dc|_{c=1}$ may be of opposite signs and the flow may be stable while the viscosity contrast is unfavorable ($\eta_2 < \eta_1$) and vice versa [55]. The stability of the flow depends, not on the end-point viscosities, but on the end-point derivatives of the viscosity with respect to concentration. This situation is of particular interest in the case of water–methanol mixtures. Therefore, when a sample dissolved in a water–methanol mixture of a given composition is injected in a water–methanol mixture of another composition, a VF instability will develop at that interface for which the stability criterion (12) is not satisfied. However, the location of the unstable interface (leading edge or tailing edge) may not be that governed by relation (8).

2.4. Rate of change of the perturbation

The simplified model depicted in Fig. 1 and discussed in Section 2.1 allows to get some description about the evolution of the perturbation. The velocities u_A and u_B represent the rate of change of the positions of the interfaces in sections A and B of the chromatographic column, respectively, and their difference represents the rate of change of the perturbation of length δz:

$$u_B - u_A = \frac{d(z+\delta z)}{dt} - \frac{dz}{dt} = \frac{d(\delta z)}{dt} \tag{13}$$

Letting $\rho_1 = \rho_2$ in Eq. (6), one gets:

$$\frac{d(\delta z)}{dt} = -\frac{u_B}{L_c}\frac{(\eta_2 - \eta_1)\delta z}{[\eta_2(z/L_c) + \eta_1(1-(z/L_c))]} \tag{14}$$

The rate of change of the perturbation appears to be approximately proportional to the perturbation itself. For small perturbations, Eq. (14) gives:

$$\delta z = A_p \exp\left[-\frac{u_B}{L_c}\frac{(\eta_2/\eta_1) - 1}{1 + ((\eta_2/\eta_1) - 1)(z/L_c)}t\right] \tag{15}$$

where A_p is the initial amplitude of the perturbation at time $t = 0$. This equation is valid only at small times for which the position of the interface has not changed significantly after the onset of the perturbation. Nevertheless, in spite of these limitations and of the simple VF model depicted in Fig. 1, it illustrates the exponential behavior of the initial evolution of the perturbation. When the argument of the exponential term is negative, i.e. when $\eta_2 > \eta_1$, the perturbation decays exponentially with time, while it grows exponentially with time if the displacing fluid is less viscous than the displaced fluid. The consequences of this exponential behavior will be exploited in a later section.

2.5. Some relevant parameters of the viscous fingering problem in chromatographic columns

Potentially, this viscous fingering instability is always present in liquid chromatography when the viscosity of the injected sample is different from that of the carrier liquid. For a monotonic viscosity vs. concentration profile, the instability is going to develop at the tail of the peak if the sample is more viscous than the eluent, and at the front of the peak in the opposite case.

Clearly, as seen from Eq. (14) for a monotonic viscosity versus concentration profile, the motor for this instability is the viscosity contrast between the two fluids. As soon as $\eta_1 \neq \eta_2$, a viscous fingering instability will amplify any little perturbation of the interface because of a mobility difference across the interface, the less viscous fluid traveling faster than the more viscous one. The fastest moving fluid is therefore crashing into the slow moving one, "destroying" the planar interface. Eq. (15) reveals that the parameter measuring the efficiency of this destabilizing mechanism is the viscosity ratio, η_2/η_1 (or the relative viscosity difference, $\eta_2/\eta_1 - 1$) rather than the absolute viscosity difference. As soon as $\eta_1 > \eta_2$ the less viscous fluid displaces the more viscous one and fingering starts. When $\eta_1 = \eta_2$, the two fluids have the same viscosity, the various dispersion mechanisms (molecular diffusion, eddy diffusion and, possibly, mass transfer between phases) are the only transport phenomena that will mix the interface which remains planar. When η_1/η_2 is increased, the viscosity difference increases as well and hence the more unstable becomes the system.

A second important parameter of the problem is the flow velocity, u, related to the imposed pressure drop along the column or imposed flow rate. Eq. (15) indicates that the rate of growth of the instability, at its onset, increases with increasing flow velocity.

The instability mechanism explained in the previous section shows that any little perturbation should grow as soon as $\eta_1/\eta_2 > 1$ whatever its characteristic width along the planar interface. As a matter of fact, in a homogeneous porous medium, the pattern emerging at the onset of VF is usually characterized by a well defined intrinsic width of the fingers which is the result of a compromise between the destabilizing viscosity contrast and a stabilizing mechanism which has to be present for limiting the finger growth since this growth cannot realistically be indefinitely exponential. For immiscible fluids, the stabilizing action is provided by the interfacial tension since the finger growth is accompanied by a large increase in the interfacial surface area, which is energetically unfavorable. In the case of miscible fluids, of interest in chromatography, this stabilizing action is provided by the dispersion mechanism, both axial dispersion, for dampening the axial concentration gradient and hence the axial viscosity gradient which is driving VF, and transverse dispersion, for dampening the transverse concentration unequalities which are the manifestation of the presence of fingers and, hence, for homogenizing the fingers perpendicularly to the flow direction. All perturbations of very narrow width will immediately be smoothed out by transverse band broadening. It is only above a given critical finger width that dispersion is not effective enough on the time scales of the fingering instability to kill the perturbations due to the viscosity difference. The value of this critical width will depend on the ratio, ε, between transverse and axial dispersion which is thus also a key parameter of the problem. As it is known that axial and transverse dispersions do not depend in the same way on the flow velocity, ε also depends on u. There-

fore, the effect of u on the VF pattern is not as straightforward as implied by Eq. (15).

Viscous fingering will hence depend essentially on three parameters i.e. the viscosity ratio η_2/η_1, the flow velocity u, and the ratio ε between transverse and axial dispersion coefficients. Our objective is here to gain insight on the influence of each of these parameters on the width of the fingers that appear at the onset of the instability. It can be noted that, in the present context, the expressions "dispersion" and "dispersion coefficient" encompass the various mechanisms other than viscous fingering leading to band broadening, in both axial and transverse directions.

3. Linear stability analysis

A linear stability analysis (LSA) is a mathematical treatment of a stability problem that allows to describe the characteristics of the instability in the early stages of its development. Such a treatment is very general and has been applied to a large number of situations where flow instabilities occur [56,57]. In this section, we describe the main features of a LSA, and we present the main results of the LSA of the viscous fingering problem in a porous medium performed by Tan and Homsy [1]. This analysis relies on a model describing the flow and mass transport in the column. The basic equations of this model are first described below.

3.1. Basic equations of the model

We consider that the column is homogeneously packed and has a constant permeability, k_p. The local flow velocity is assumed to be related to the local pressure gradient according to the Darcy law in the flow direction, z, as well as in the transverse directions, x and y:

$$v_x = -\frac{k_p}{\eta}\frac{\partial P}{\partial x} \tag{16a}$$

$$v_y = -\frac{k_p}{\eta}\frac{\partial P}{\partial y} \tag{16b}$$

$$v_z = -\frac{k_p}{\eta}\frac{\partial P}{\partial z} \tag{16c}$$

where v_x, v_y and v_z are the components of the local flow velocity vector along the corresponding directions, x, y and z, P is the local pressure and η the local value of the fluid viscosity. At this point, there is no need to specify which kind of flow velocity (superficial, chromatographic, or interstitial velocity) is involved as the proportionality coefficients between these three quantities are assumed to be constant throughout the column [58a]. The concept of local property must be here understood as corresponding to a region of volume at least equal to the representative elementary volume for which the continuum approach can be applied to the porous medium [9c]. For homogeneous packings of uniform spheres, this corresponds to a length scale of approximately five particle sizes [59].

The continuity equation, which expresses mass conservation of the fluids is written, for uncompressible fluids, as:

$$\frac{\partial v_x}{\partial x} + \frac{\partial v_y}{\partial y} + \frac{\partial v_z}{\partial z} = 0 \tag{17}$$

Let us follow the evolution in a porous medium of one single planar interface between two miscible fluids traveling along the z direction and the viscosity of which depends on the concentration c of the displaced fluid 1. The evolution of the composition of the mixture of the two fluids 1 and 2 is therefore described by a convection–diffusion equation for c:

$$\frac{\partial c}{\partial t} + v_x\frac{\partial c}{\partial x} + v_y\frac{\partial c}{\partial y} + v_z\frac{\partial c}{\partial z} = D_{ax}\frac{\partial^2 c}{\partial z^2} + D_{tr}\left(\frac{\partial^2 c}{\partial x^2} + \frac{\partial^2 c}{\partial y^2}\right) \tag{18}$$

D_{ax} and D_{tr} are the axial and transverse dispersion coefficients, respectively. The dispersion process is assumed isotropic in the transverse directions x and y. However, because they depend differently on the axial flow velocity, D_{ax} and D_{tr} may be significantly different. They are assumed constant throughout the column. It should be noted that the mass conservation equation for the downstream fluid accounts solely for its concentration c in the liquid mixture. Hence, it is implicitly assumed that there is no adsorption or distribution within the stationary phase involved in the present theory. The crucial question of the influence of retention on the VF phenomenon will be treated in forthcoming publications. The present theory can be applied only to unretained species.

The local viscosity entering Eq. (16) is that of the mixture of fluids. Eqs. (16–18) must therefore be completed by an expression of the dependence of η on c. There are various equations describing such a dependence [60]. In this study, the empirical Arrhenius expression for the viscosity is used [61]. It states that the logarithm of the viscosity of the mixture is the sum of the logarithms of the viscosities of the individual components weighted by their relative amounts in the mixture. This law is found satisfying if this relative amount is selected as the mole fraction [62]. Thus, if the mole fraction of the displaced fluid (fluid 1 in Fig. 1) in the binary fluid mixture is taken as the concentration unit c in Eq. (18), the Arrhenius expression is written as:

$$\ln\eta = c\ln\eta_1 + (1-c)\ln\eta_2 \tag{19}$$

or, equivalently:

$$\ln\frac{\eta}{\eta_2} = Rc \tag{20}$$

with

$$R = \ln\frac{\eta_1}{\eta_2} \tag{21}$$

The logmobility ratio, R, can be considered as the key parameter driving the VF instability. The viscosity–concentration profile described by Eqs. (19) or (20) is monotonic. Therefore, the condition for stability is $\eta_2 > \eta_1$, or $R < 0$. As noted earlier, Eqs. (19) or (20) do not apply for water–methanol and water–acetonitrile mixtures which exhibit a maximum viscosity at some intermediate composition [58b].

In order to solve the system of Eqs. (16–19), the initial conditions must be defined. We assume that the sample is introduced in the packed column as a rectangular plug surrounded by the mobile phase. The length initially occupied by the sample at the time of introduction is an important parameter of the problem. However, as, in this study, we are interested by what happens at the beginning of the development of the VF instability, we are mainly concerned by that sample-mobile phase interface which is unstable. As seen in Section 2.1, this is the upstream interface if the sample is more viscous than the carrier liquid (then fluid 1 is the sample, and fluid 2 the carrier), the downstream interface in the opposite case (then fluid 1 is the carrier and fluid 2 the sample). Therefore, the length of the sample plug, L_{inj}, is not a pertinent parameter in the present study and we will consider that fluids 1 and 2 extend semi-infinitely on each side of the unstable interface. Thus, the conclusions of this approach can be considered as correct only when there is still a constant sample concentration plateau between the front and rear interfaces. They cannot be applied to the real chromatographic situation when the two interfaces of the sample plug start to interact under the effect of dispersion, i.e. when the standard deviation of each interface becomes larger than about $L_{\text{inj}}/4$, hence at times larger than about $L_{\text{inj}}^2/(32D_{\text{ax}})$.

To simplify the study in this first approach to VF, we consider the situation of an unretained sample (this is why there is no term containing the sample concentration in the stationary phase in Eq. (18)) and leave the influence of retention on VF to a later study. If we assume that the interface is a step function in concentration centered at $z=0$ at time 0, and that a constant flow rate, corresponding to a constant velocity u along the z-direction, of the displacing fluid is introduced in the system, then the solutions of Eqs. (16–19) are:

$$v_{x,o} = 0 \tag{22a}$$

$$v_{y,o} = 0 \tag{22b}$$

$$v_{z,o} = u \tag{22c}$$

$$c_o(z,t) = \frac{1}{2}\left[1 + \text{erf}\left(\frac{z-ut}{2\sqrt{D_{\text{ax}}t}}\right)\right] \tag{23}$$

$$\eta_o(z,t) = \eta_2 \exp[Rc_o(z,t)] \tag{24}$$

$$P_o(z,t) = -\frac{u}{k_{\text{p}}}\int^z \eta_o(z',t)\,\text{d}z' \tag{25}$$

where erf is the error function [63]. The subscripts "o" appearing in Eqs. (22–25) indicate that the values of the parameters correspond to the base state, i.e. that state obtained in absence of any flow instability. The base state concentration profile given by Eq. (23) is that which is observed in frontal analysis. It does not depend on the transverse coordinates and has a characteristic sigmoidal shape along the flow axis. It induces a base state viscosity profile, $\eta_o[c_o(z,t)]$, obtained from Eqs. (23) and (24), and a corresponding base state pressure profile given by Eq. (25). Because of the axial dispersion process, the base state concentration, viscosity and pressure profiles are time dependent. It can be noted that, in order to obtain the pressure profile from Eq. (25), a reference pressure is needed. In practice, this is the atmospheric pressure at column outlet. However, because the column length is not a relevant parameter in the LSA, this is not specified in Eq. (25).

3.2. Principles of linear stability analysis

The principle of a LSA is to see whether small perturbations around the base state of Eqs. (22–25) will be amplified or not in the course of time. It consists in writing the various quantities, q, of the model (i.e. v_x, v_y, v_z, P, c, η) as:

$$q = q_o + q' \tag{26}$$

where the q_o quantities are the base state quantities (here given by Eqs. (22–25) while the q' are small fluctuations from the base state. Inserting Eq. (26) for each of the model variable into the basic model Eqs. (16–19), assuming that the perturbations are small enough for all nonlinear terms in the perturbations to be neglected, and combining the resulting equations with the base state expressions (22–25) gives a system of linear partial differential equations describing the linearized evolution of the perturbations q'.

A key feature of a LSA is to recognize that, near their onset, the perturbations have a wavy, periodic pattern that propagates along the flow direction z. Therefore, one seeks solutions of the linear partial differential equations for the quantities q' that have a sinusoidal shape in the transverse directions x and y, that are hence written as:

$$q' = \Phi(z,t)\text{e}^{ik_x x}\text{e}^{ik_y y} \tag{27}$$

where the amplitude Φ varies with the particular quantity q' at hand (for example, a concentration or an axial velocity) and has the dimension of this quantity. It is a function of the axial position z and of the time t. i is the imaginary unit, k_x and k_y are the wavenumbers of the disturbances in the directions x and y. Another key feature of a LSA is to express that the amplitude Φ depends exponentially on time:

$$\Phi(z,t) = \phi(z,0)\text{e}^{\omega t} \tag{28}$$

where ω is the growth rate of the instability. Selecting such an evolution law for the instability is justified on the ground of many experimental observations of the various kinds of instabilities. This expresses that the rate of change of the amplitude of a perturbation is proportional to this amplitude. In our simple model describing the mechanism of VF, such an exponential evolution law has been obtained in Section 2.4 (see Eq. (15)).

Setting Eqs. (27) and (28) into the system of partial differential equations describing the evolution of the perturbations allows to eliminate the quantities q' and to obtain a relationship between the growth rate ω and the wavenumber k defined as:

$$k = \sqrt{k_x^2 + k_y^2} \tag{29}$$

Such a relationship allows to derive the wavenumbers (and associated wavelengths, connected to the finger widths) which have the largest positive growth rate ω and are thus growing the fastest. It is the main result of a LSA. In the field of wave theory, the ω

versus k relationship is commonly called the "dispersion relation" [1,56,57,64]. It should be noted that the term "dispersion" in this context is used to distinguish "dispersive" waves from "non-dispersive" waves for which ω/k is constant whatever k. This term is without connection with the usual meaning that it has in the chromatographic context where it is associated with the band broadening process.

A particular characteristic of instabilities involving miscible fluids is that the base state is not translated unchanged along the flow direction as time elapses, because of the diffusion or dispersion processes. Such a time dependence of the base state, due to the axial dispersion, is apparent from Eq. (23). This somewhat complicates the derivation of the dispersion relation. In their LSA study on miscible displacements in porous media, Tan and Homsy [1] solved this difficulty by applying the quasi-steady-state approximation, which assumes that the growth rate of the disturbances is much faster than the rate of change of the base state. With this approximation, taking the base state as frozen at a given time t_o, ω and ϕ in Eq. (28) should be considered as dependent on t_o.

3.3. Linear stability analysis of the VF instability in a porous medium

The LSA of the VF instability in a porous medium was first derived by Chouke assuming a step viscosity profile, a linear viscosity–concentration relationship, and an isotropic dispersion (i.e. $D_{ax} = D_{tr}$) [65]. Tan and Homsy extended the calculations to the more realistic situation, in the liquid chromatographic context, of a viscosity profile given by Eq. (19) and of anisotropic dispersion [1]. To do this, Eqs. (20–33) are rendered dimensionless by selecting reference values of length and time. Because the geometrical lengths of the chromatographic columns are not relevant parameters in the LSA, the reference time and length are defined by means of the physical parameters entering the model as:

$$L_{ref} = \frac{D_{ax}}{u} \tag{30}$$

and

$$t_{ref} = \frac{L_{ref}}{u} = \frac{D_{ax}}{u^2} \tag{31}$$

Tan and Homsy [1] obtained an analytical expression of the dispersion relation for the basic model described in Section 3.1 at time 0, i.e. when the unstable interface is a step profile. Their result is expressed in terms of dimensionless quantities, ω^* for the dimensionless growth rate and k^* for the dimensionless wavenumber:

$$\omega^* = \frac{1}{2}\left[(Rk^* - k^{*2}) - k^*\sqrt{k^{*2} + 2Rk^*}\right] + (1-\varepsilon)k^{*2} \tag{32}$$

In the following, dimensionless quantities are denoted with "*". The dimensional growth rate and wavenumber are:

$$\omega = \frac{\omega^*}{t_{ref}} = \omega^* \frac{u^2}{D_{ax}} \tag{33}$$

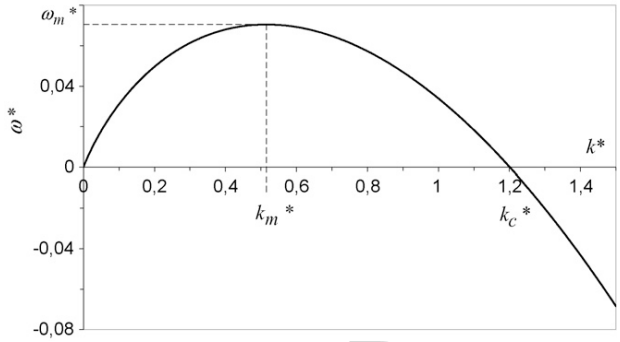

Fig. 2. Dimensionless dispersion relation, ω^* vs. k^*, at time 0, of the viscous fingering phenomenon occurring in a porous medium at a step interface between an upstream liquid 2 less viscous than a miscible downstream liquid 1, according to Eq. (37) for $R = 1$ and $\varepsilon = 0.1$.

and

$$k = \frac{k^*}{L_{ref}} = k^* \frac{u}{D_{ax}} \tag{34}$$

To any wavenumber, k or k^*, is associated a wavelength, λ or λ^*:

$$\lambda = \frac{2\pi}{k} \tag{35a}$$

or

$$\lambda^* = \frac{2\pi}{k^*} \tag{35b}$$

In Eq. (32), the parameter ε is the dispersion ratio, defined as:

$$\varepsilon = \frac{D_{tr}}{D_{ax}} \tag{36}$$

It measures the anisotropy of the dispersion process.

The dispersion relation (32) contains the searched informations about the response of the chromatographic system to any kind of disturbances, since it provides the values of the growth rate ω of the exponential increase of a given perturbation as a function of its wavenumber. It is noticeable that the dispersion relation (32) depends only on a few parameters when written in dimensional terms. These parameters are the flow velocity, u, the axial dispersion coefficient, D_{ax} (these two parameters are involved in the definition of the reference length and time), the transverse dispersion coefficient, D_{tr} (through the dispersion ratio, ε), and the viscosity contrast (through the logmobility ratio, R). It does not explicitly depend on the column permeability. Nevertheless, the particle size influences the VF process through its effect on the dispersion coefficients.

3.4. Characteristics of the dispersion relation

The dispersion relation obtained from Eq. (32), for $R = 1$ (i.e. $\eta_1/\eta_2 = 2.72$) and $\varepsilon = 0.1$, is shown in Fig. 2. This curve is typical of many dispersion relations obtained in various situations where flow instabilities occur.

First, it is seen that there is a range of wavenumbers for which ω is positive. Accordingly, the system is unstable with regard to the viscous instability since all disturbances with these

wavenumbers will be exponentially amplified as time elapses. In fact, Fig. 2 illustrates that the unstable range of wavenumbers extends from 0 to a cut-off k_c^*. Modes with wavenumbers larger than the critical or cut-off wavenumber k_c^* lead to negative ω values, and, thus, are stable. In other words, modes with wavelengths smaller than a critical value cannot develop themselves, but will decay exponentially. Physically, this illustrates the fact that fingers which are too narrow are immediately smoothed out by transverse dispersion.

The curve of Fig. 2 exhibits a maximum growth rate, ω_m or ω_m^*, for a particular value of the wavenumber, k_m or k_m^*. This corresponds to the mode which will grow the fastest. This mode is called the most probable mode as this is the mode which will eventually dominate the other ones, or also, the most dangerous mode, as this is the most unstable one. In practice, the finger width, if measured as the average distance between the tips of two neighbor fingers at onset corresponds therefore to λ_m, i.e. $2\pi/k_m$. The characteristic onset time, τ, of the pattern is given as $\tau = 1/\omega_m$. The LSA allows therefore to have insight on both the characteristic wavelength and the onset time of the VF pattern.

3.5. Influence of the dispersion ratio

Dividing the two sides of Eq. (32) by R^2 shows that the analytical dispersion relation computed for $t = 0$, for which the base state is a step function, can be expressed as:

$$\frac{\omega^*}{R^2} = \frac{1}{2}\left(\frac{k^*}{R}\right)\left[1 - \left(\frac{k^*}{R}\right) - \sqrt{\left(\frac{k^*}{R}\right)^2 + 2\left(\frac{k^*}{R}\right)}\right] + (1-\varepsilon)\left(\frac{k^*}{R}\right)^2 \quad (37)$$

Eq. (37) shows that a plot of ω^*/R^2 versus k^*/R only depends on the dispersion ratio ε. Thus the characteristic wavenumbers (k_c^* and k_m^*) are scaled to R while the maximum growth rate is scaled to R^2. It is easily shown that the cut-off value is:

$$\frac{k_c^*}{R} = \frac{\sqrt{(1/\varepsilon)} - 1}{2(1-\varepsilon)} \quad (38)$$

It is seen that, as $\varepsilon \to 0$ (very strong dispersion anisotropy), k_c^*/R increases as $1/\sqrt{4\varepsilon}$, while its limit when $\varepsilon \to 1$ (isotropic axial and transverse dispersion) is:

$$\lim_{\varepsilon \to 1}\left(\frac{k_c^*}{R}\right) = \frac{1}{4}\left[1 + \frac{3}{4}(1-\varepsilon)\right] \quad (39)$$

The most probable wavenumber is solution of:

$$8\varepsilon(1-\varepsilon)\left(\frac{k_m^*}{R}\right)^3 + 4\varepsilon(5-4\varepsilon)\left(\frac{k_m^*}{R}\right)^2 + 8\varepsilon\left(\frac{k_m^*}{R}\right) - 1 = 0 \quad (40)$$

The dispersion relations, for various values ε, are plotted in Fig. 3 as ω^*/R^2 versus k^*/R. The curves have a similar aspect. Still, it is seen that, as ε decreases, the growth rate, for a given k^*, increases. Furthermore, in the same time, the cut-off and most dangerous wavenumbers increase and the maximum growth rate also increases. These wavenumber and growth rate variations with ε are shown in Figs. 4 and 5, respectively. That k_c^* decreases with increasing ε reflects the fact that as the tranverse dispersion becomes more important, neighbor fingers of narrow widths (i.e.

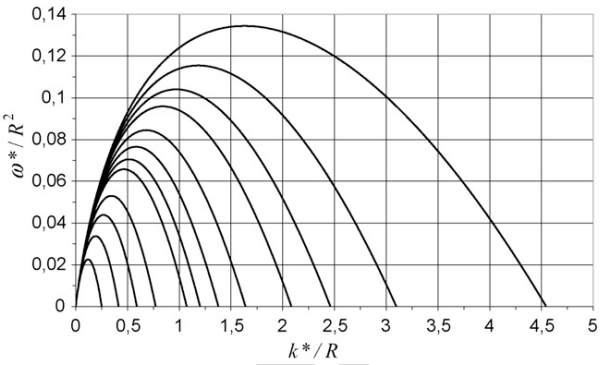

Fig. 3. Dimensionless dispersion relation, ω^*/R^2 vs. k^*/R, at time 0, of the viscous fingering phenomenon occurring in a porous medium at the step interface between a low viscosity liquid displacing a high viscosity miscible liquid, for various values of the dispersion ratio ε. From the lower to the upper curves: $\varepsilon = 1$; 0.5; 0.3; 0.2; 0.12; 0.10; 0.08; 0.06; 0.04; 0.03; 0.02; 0.01.

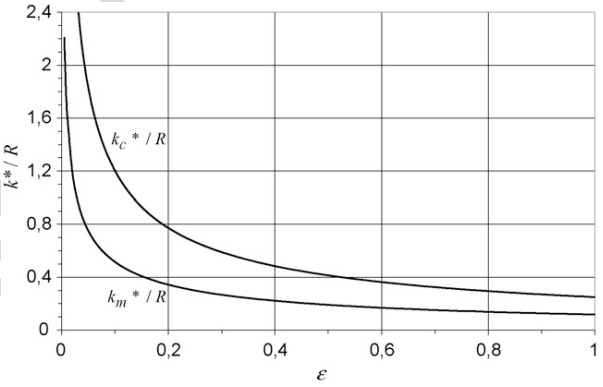

Fig. 4. Dimensionless most probable and cut-off dimensionless wavenumbers per unit value of the viscosity contrast parameter R, k_m^*/R and k_c^*/R, respectively, vs. dispersion ratio, ε, for viscous fingering, at time 0, at the step interface between a low viscosity liquid displacing a high viscosity miscible liquid.

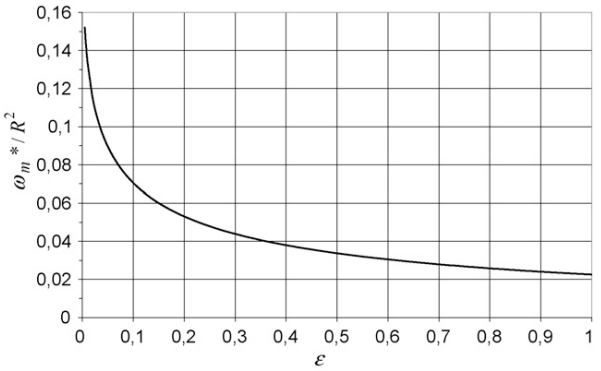

Fig. 5. Maximum dimensionless growth rate per unit value of the square of the viscosity contrast parameter R, ω_m^*/R^2, vs. dispersion ratio, ε, for viscous fingering, at time 0, at the step interface between a low viscosity liquid displacing a high viscosity miscible liquid.

of large wavenumbers) cannot survive individually because they are quickly smoothed out by dispersion.

A close inspection to Eq. (32) shows that for large wavelengths, i.e. when $k \to 0$, the dominant term is linearly proportional to R. This means that genuinely the origin of the instability, in absence of any dispersion smoothing out small length scales (or equivalently large k), is the viscosity ratio between the two fluids. If the displacing fluid is more viscous than the displaced one, $R<0$ and the growth rate is negative, hence the system is stable. If the displacing fluid is the less viscous one, $R>0$ and an instability occurs with an intensity linearly proportional to the viscosity ratio. Transverse dispersion counteracts this instability by smoothing out any small perturbation, hence providing a negative stabilizing term proportional to εk^2 in the dispersion relation. Axial dispersion is also a stabilizing mechanism: initially we have a sharp interface, but axial dispersion causes this jump to spread out in time thus diminishing the viscosity gradient across the interface in time.

4. Application to liquid chromatography

The main result of the LSA of the VF phenomenon in a porous medium is the dispersion relation expressed by Eq. (37). It is given in dimensionless terms. In this section, we translate this expression into usual quantities characterizing the chromatographic process. The relationship between ω^* and k^* depends on two parameters, R and ε. According to Eq. (21), R is the natural logarithm of the viscosity ratio. Hence, R-values of 0.5, 1 and 2 correspond to viscosity ratios of 1.6, 2.7, and 7.4, respectively. ε is the dispersion ratio, defined by Eq. (36). Its typical values in liquid chromatography, as well as those of the reference length and time required to expressed the growth rate and finger width (or wavelength) in dimensional quantities, are discussed in the next section.

4.1. Dispersion ratio in LC

The axial and transverse dispersion coefficients, D_{ax} and D_{tr}, are related to the axial and transverse (radial) plate heights, H_{ax} and H_{tr}, as:

$$D_{ax} = \frac{H_{ax}u}{2}; \tag{41a}$$

$$D_{tr} = \frac{H_{tr}u}{2} \tag{41b}$$

The chromatographic literature makes frequent use of dimensionless parameters, the reduced velocity, ν, and the reduced (axial) plate height, h_{ax}, defined as [66]:

$$\nu = \frac{ud_p}{D_m} \tag{42}$$

and

$$h_{ax} = \frac{H_{ax}}{d_p} \tag{43}$$

where D_m is the molecular mutual diffusion coefficient of the sample in the carrier liquid and d_p is the average particle size of the porous bed. Similarly, the reduced transverse plate height, h_{tr}, can be defined as:

$$h_{tr} = \frac{H_{tr}}{d_p} \tag{44}$$

These dimensionless quantities are nothing else than some Péclet numbers (or reciprocals of Péclet numbers) based on flow velocity, particle size (or half this size), and either D_m, D_{ax} or D_{tr}, for the diffusivity.

Combining Eqs. (30), (41a) and (43) shows that the reference length and time are equal to:

$$L_{ref} = \frac{1}{2}H_{ax} \tag{45}$$

and

$$t_{ref} = \frac{1}{2}\frac{H_{ax}}{u} \tag{46}$$

Eq. (45) shows that the reference length is half the axial plate height. The reference time is the transit time over a distance of half a plate. It is seen from Eqs. (36) and (41–44) that the dispersion ratio ε is equal to:

$$\varepsilon = \frac{H_{tr}}{H_{ax}} = \frac{h_{tr}}{h_{ax}} \tag{47}$$

The axial and transverse plate heights depend on various flow, porous bed and analyte parameters. There have been several theories and correlations developed to express these dependences, both in the chromatography field and in the chemical engineering, petroleum engineering, soil science and physics field. For reviews of these investigations, see Refs. [58c,67,68] for the chromatography field, and [69,70] for the engineering and physics field. In many cases, dispersion studies in one field ignored the studies in the other field. This probably comes, in part, from the different terminology used by these communities. Chromatographers use the unfortunate, but widespread, expression "plate height" or "height equivalent to a theoretical plate" to describe the quantity H_{ax}, after the seminal work of Martin and Synge [71], while physicists use the more meaningful term "dispersion length" to describe the quantity L_{ref}, which as seen from Eq. (45) is half the plate height.

Porous beds in modern LC have some peculiarities compared to porous media involved in engineering. LC columns are homogeneously packed with quasi-monodisperse spherical particles of very narrow size. Accordingly, for separation optimization purposes as well as because of pressure limitations, they are operated in a relatively narrow range of reduced velocities, typically between 2 and 30. This is a ν region where the coupling of molecular diffusion and anastomosis (i.e. the crossing of streamlines, or stream-splitting, in a porous medium combined with velocity fluctuations along a streamline), described by Giddings [72], is dominantly controlling the eddy diffusion (as it is called in the chromatography literature) or hydrodynamic dispersion (as it is called in the physics literature) contribution to band broadening in the mobile phase. Therefore, in order to express the dependence of the plate height on the operating parameters, we prefer to use the so-called "Knox equation", which is well

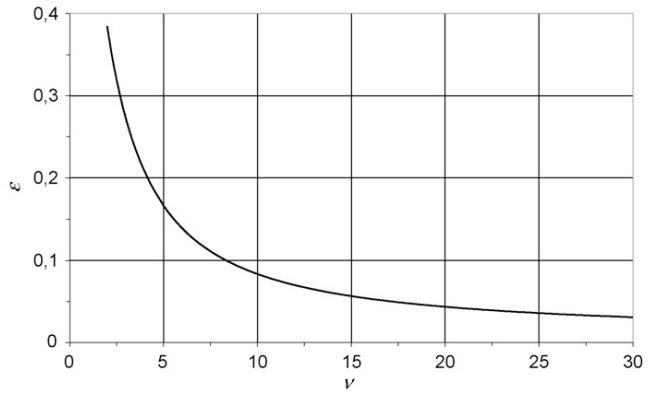

Fig. 6. Dispersion ratio, ε, vs. reduced velocity, ν, for typical values of the plate height parameters, $A=1$, $B=D=1.4$, $C=0.01$, $E=0.06$.

adapted to the description of dispersion in the ν range of interest in LC rather than other correlations of wider scope found in the engineering literature (see Ref. [70]). In dimensionless parameters, this semi-empirical equation is written as [73]:

$$h_{ax} = \frac{B}{\nu} + A\nu^{1/3} + C\nu \tag{48}$$

where A, B and C are dimensionless constants.

The transverse plate height also depends on the operating parameters. There is a general agreement, in the fields of chromatography as well as of engineering and physics, that this dependence is expressed as:

$$h_{tr} = \frac{D}{\nu} + E \tag{49}$$

where D and E are dimensionless constants. For isotropic materials, D should be equal to B. The measurement of transverse dispersion is more difficult than that of axial dispersion. This is why there are very few determinations of D and E in LC columns [74–76], as well as in engineering systems [69,70]. Reported values of E are equal to 0.11 [69], 0.17 [70], 0.060 [74], 0.075 [75] and 0.12 [76].

Eqs. (48) and (49) show that the flow rate dependences of the axial and tranverse dispersion coefficients are different. Accordingly, their ratio ε depends on flow velocity. This dependence is shown in Fig. 6 for typical values of the dimensionless constants, $A=1$, $B=D=1.4$, $C=0.01$ and $E=0.06$. These values are typical for unretained species [73,74]. It is seen, on Fig. 6, that the dispersion ratio, in typical LC conditions, is well smaller than 1. It decreases steadily as the reduced velocity increases, which reflects the fact that the axial dispersion coefficient increases faster with the reduced velocity than the transverse dispersion coefficient does.

4.2. Dispersion relation versus flow velocity

The dispersion relation is shown on Fig. 7 for various values of ν, from 2 to 30. It is seen that the larger ν, the larger the dimensionless growth rate for any dimensionless wavenumber. It is seen on Fig. 8 that the most dangerous and the cut-off

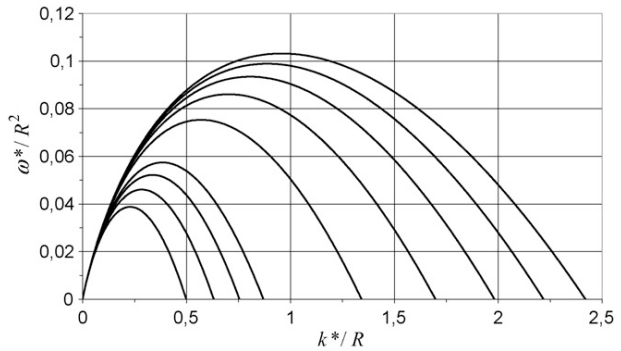

Fig. 7. Dimensionless dispersion relation, ω^*/R^2 vs. k^*/R, at time 0, of the viscous fingering phenomenon occurring in a porous medium between a step interface between an upstream liquid 2 less viscous than a miscible downstream liquid 1, for various values of the reduced velocity. From the lower to the upper curves: $\nu=2$; 3; 4; 5; 10; 15; 20; 25; 30.

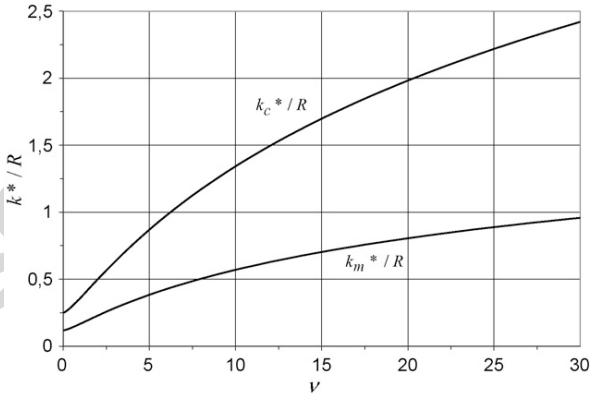

Fig. 8. Dimensionless most probable and cut-off dimensionless wavenumbers per unit value of the viscosity contrast parameter R, k_m^*/R and k_c^*/R, respectively, vs. reduced velocity, ν, for viscous fingering, at time 0, at the step interface between a low viscosity liquid displacing a high viscosity miscible liquid.

wavenumbers increase steadily with ν. Similarly, on Fig. 9, the maximum growth rate, ω^* is found to increase with ν. The values observed in the limit of $\nu=0$ correspond to the hypothetical situation where the axial and transverse dispersion coefficients are

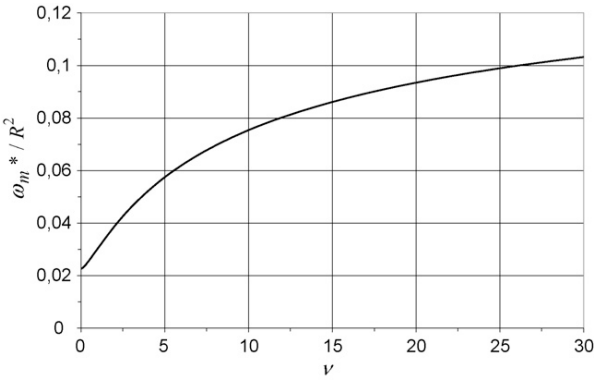

Fig. 9. Maximum dimensionless growth rate per unit value of the square of the viscosity contrast parameter R, ω_m^*/R^2, vs. reduced velocity, ν, for viscous fingering, at time 0, at the step interface between a low viscosity liquid displacing a high viscosity miscible liquid.

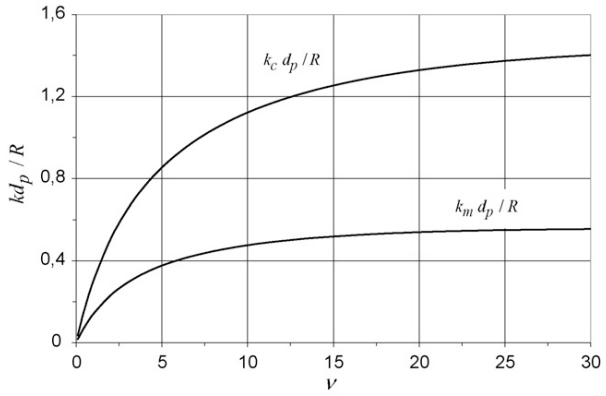

Fig. 10. Most probable and cut-off wavenumbers per unit value of the viscosity contrast parameter R, related to the particle diameter, $k_m d_p/R$ and $k_c d_p/R$, respectively, vs. reduced velocity, ν, for viscous fingering, at time 0, at the step interface between a low viscosity liquid displacing a high viscosity miscible liquid.

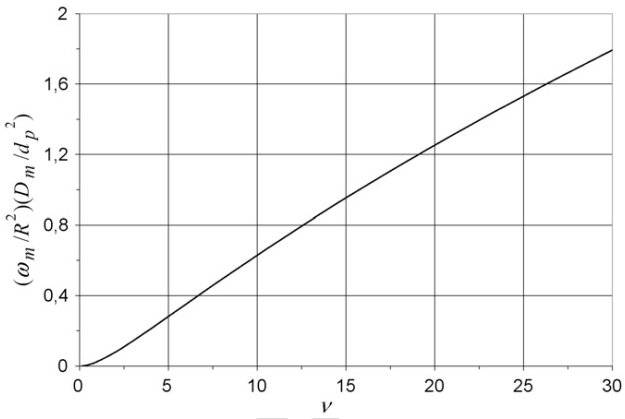

Fig. 11. Maximum growth rate, (ω_m/R^2) (D_m/d_p^2), per unit value of the square of the viscosity contrast parameter R, related to the diffusion time across one particle, D_m/d_p^2, vs. reduced velocity, ν, for viscous fingering, at time 0, at the step interface between a low viscosity liquid displacing a high viscosity miscible liquid.

equal ($\varepsilon = 1$), i.e. $k_c^*/R = 1/4$, $k_m^*/R = (\sqrt{5}/2) - 1 \approx 0.118$, and $\omega_m^*/R^2 = (5\sqrt{5} - 11)/8 \approx 0.0225$ [1].

The curves shown on Figs. 8 and 9 represent variations of the dimensionless quantities, k^* and ω^*, as a function of the reduced velocity. However, as these dimensionless quantities themselves depend on ν through L_{ref} and t_{ref}, it is interesting to investigate the dependence of the dimensional quantities ω and k on the flow velocity. From Eqs. (33), (34) and (41–43), it comes:

$$\frac{k}{R} = \frac{2}{h_{ax}} \frac{k^*}{R} \frac{1}{d_p} \tag{50}$$

and

$$\frac{\omega}{R^2} = \frac{2\nu}{h_{ax}} \frac{\omega^*}{R^2} \frac{D_m}{d_p^2} \tag{51}$$

The variations of $k_m d_p/R$ and of $k_c d_p/R$ as functions of the reduced velocity are shown in Fig. 10, and those of $(\omega_m/R^2)(d_p^2/D_m)$ versus ν in Fig. 11.

The wavenumbers k_c and k_m are seen to increase with increasing ν in the ν range shown in Fig. 10, but the slopes of the curves decrease as ν increases. In fact, it can be shown that both wavenumbers reach maximum values, which are $k_c d_p/R = 1.435$ for $\nu = 51$, and $k_m d_p/R = 0.556$ for $\nu = 35$. Instead, the perturbation growth rate increases steadily with increasing ν as seen in Fig. 11. This increase is almost linear in the ν range of interest. It is interesting to note that, in the simple model depicting the VF phenomenon in Section 2, the growth rate appears to be linearly proportional to the flow velocity as seen in Eq. (15). Therefore, when the perturbations are still small enough for their evolution to be described Eq. (28), i.e. when nonlinear terms are negligible, their amplitude is nearly independent of the flow velocity (since ω is nearly proportional to u and $t = z/u$) and they grow as e^z with the distance z traveled by the interface.

It is interesting to give some numbers for the characteristic parameters at the onset of the VF instability for typical operating conditions of an analytical LC column. The parameters selected for describing the chromatographic system, the derived flow and dispersion parameters, the corresponding reference dimensions, and the VF characteristic parameters are reported in Table 1. The numbers of the equations used to compute these quantities are also given. It is seen that the reference parameters are quite small, 6.67 μm for the length and 4.66 ms for the time. This reflects the high efficiency of the chromatographic system since the reference length is half the axial plate height, and the reference time the transit time over that distance. The VF parameters are given for three values of the viscosity ratio, η_1/η_2, and hence of the logmobility ratio, R. The intermediate values correspond to $R = 1$, i.e. to $\eta_1/\eta_2 = 2.72$. The other values correspond to a two-times smaller and a two-times larger viscosity ratio. It is seen that the wavenumbers are large, of the order of 100 or 1000 cm^{-1}, which indicates that, at the onset of VF, there are of the order of 100 or 1000 undulations per cm in the transverse direction, the more so as R is larger. Their most probable wavelength is small, about 0.2 mm for a rather small viscosity ratio and still smaller for larger R-values. They correspond to the mode which grows the fastest. The characteristic time, τ_{VF}, for the growth of the instability can be defined, from Eq. (28) as:

$$\tau_{VF} = \frac{1}{\omega_m} \tag{52}$$

This is the time over which the amplitude of the instability increases by a factor $e^1 = 2.72$. This time is rather short, about half a second for the lowest viscosity ratio and 20 ms for the largest one in Table 1. It decreases as $1/R^2$ with increasing R.

5. Discussion

5.1. Time evolution of the dispersion relation

The above numerical estimations of the wavelengths and growth rates of the VF instability are based on the relation dispersion derived by Tan and Homsy [1] and expressed by Eq. (37). It should be remembered that this relation was obtained

Table 1
Values of the viscous fingering characteristic parameters for a typical LC analytical column

Given typical parameters of the system	
Column diameter	$d_c = 4.6$ mm
Flow rate	$Q = 1$ ml min^{-1}
Particle diameter	$d_p = 5$ μm
Total porosity	$\varepsilon_{tot} = 0.7$
Mutual diffusion coefficient	$D_m = 0.5\ 10^{-5}$ cm^2 s^{-1}
Plate height dimensionless coefficients	$A = 1$; $B = D = 1.4$; $C = 0.01$; $E = 0.06$ (from [72,73])
Derived flow and dispersion parameters	
Flow velocity	$u = 4Q/(\pi\varepsilon_{tot}d_c^2) = 0.143$ cm s^{-1}
Reduced velocity	$v = 14.3$ (from Eq. (42))
Reduced axial plate height	$h_a = 2.67$ (from Eq. (48))
Reduced transverse plate height	$h_{tr} = 0.158$ (from Eq. (49))
Axial dispersion coefficient	$D_{ax} = 9.56 \times 10^{-5}$ cm^2 s^{-1} (from Eqs. (41a) and (43))
Transverse dispersion coefficient	$D_{tr} = 0.565 \times 10^{-5}$ cm^2 s^{-1} (from Eqs. (41b) and (44))
Dispersion ratio	$\varepsilon = 0.0591$ (from Eq. (36))
Reference dimensions	
Reference length	$L_{ref} = 6.67 \times 10^{-4}$ cm $= 6.67$ μm (from Eqs. (43) and (45))
Reference time	$t_{ref} = 4.66 \times 10^{-3}$ s (from Eqs. (42), (43) and (46))

Viscous fingering characteristic parameters

Viscosity ratio Logmobility ratio	$\eta_1/\eta_2 = 1.36$ $R = 0.307$	$\eta_1/\eta_2 = 2.72$ $R = 1$	$\eta_1/\eta_2 = 5.44$ $R = 1.69$	Eqs.
Dimensionless cut-off wavenumber, k_c^*	0.508	1.65	2.80	(38)
Dimensionless most probable wavenumber, k_m^*	0.211	0.687	1.16	(40)
Dimensionless maximum growth rate, ω_m^*	0.00800	0.0849	0.243	(37) and (40)
Dimensional cut-off wavenumber, k_c	760 cm^{-1}	2480 cm^{-1}	4200 cm^{-1}	(50)
Dimensional most probable wavenumber, k_m	315 cm^{-1}	1030 cm^{-1}	1740 cm^{-1}	(50)
Cut-off wavelength, λ_c	82.6 μm	25.3 μm	15.0 μm	(35a)
Most probable wavelength, λ_m	199 μm	61.0 μm	36.1 μm	(35a)
Dimensional maximum growth rate, ω_m	1.72 s^{-1}	18.2 s^{-1}	52.2 s^{-1}	(51)
Characteristic VF time, τ_{VF}	0.583 s	0.055 s	0.019 s	(52)

for a step interface between the two fluids. As time elapses, the axial concentration profile becomes less steep under the influence of the axial dispersion process. The viscosity gradient across the front is thus decreasing in time. As a consequence, the base state is more and more stable with regard to VF as the motor of the instability is weakening in time. We intuitively expect that this reducing effect will affect the dispersion relation in the same direction as a reduction in the viscosity contrast, i.e. of R. Unfortunately, the complexity of the equations of the basic model does not allow to get an analytical expression of the time dependence of the dispersion relation. Nevertheless, numerical solutions have been obtained by Tan and Homsy [1]. They confirm the above expectation: it is found that k_c^*, k_m^* and ω_m^* decrease with time, as they do for a step interface when R decreases. Still, it is not possible to simply express the time dependences of these three quantities by means of Eqs. (37), (38) and (40) completed by a single decreasing function of R versus time. Nevertheless, the rate of decay of the three characteristic quantities of a dispersion relation decreases with time. This decay is rather slow after a few t_{ref} (let say, about $5t_{ref}$). In spite of this, the theoretical calculations of Tan and Homsy based on an initial step interface were in reasonably good agreement with available experimental data on the finger scale [1]. The decay of the growth rate may have been somewhat compensated by the destabilizing effect obtained when taking into account the dynamic dependence of the dispersion coefficients on the local velocity instead of on the constant mean velocity u [77,78]. Anyway, Eqs. (37)–(40) should be considered as providing upper limit values of k_c, k_m and ω_m.

5.2. Influence of the geometry of the column

The LSA has provided us with important information on the characteristic length scale of the fingers that appear at onset. The wavelength of the fingers that appear initially is given by $\lambda_m = 2\pi/k_m$ where k_m is the wavenumber of the most unstable wavenumber in the band of unstable modes ranging from $k = 0$ to the cut-off k_c above which all growth rates are negative. This 0 to k_c range of unstable wavenumbers is thus dictated by the physics of the VF process. This corresponds to a range of unstable wavelengths from λ_c to infinity.

However, the geometry of the chromatographic column dictates its own range of permitted wavelengths. The LSA approach described above relies on the assumption that Darcy law is valid for describing the flow inside the column. As noted in Section 3.1, this is possible if one regards the porous medium with a scale larger than the size, λ_μ, of the representative elementary volume, above which the microscopic details of the packing are smoothed. This fixes an upper limit, $k_\mu = 2\pi/\lambda_\mu$, to the permitted wavenumbers. On the other side of the spectrum, only fingers

with a wavelength smaller than the column diameter d_c will be observed, which fixes a lower geometrical cut-off wavenumber $k_g = 2\pi/d_c$ below which all unstable wavenumbers cannot be excited. For the typical analytical column considered in Table 1, assuming $\lambda_\mu = 5d_p$ [59], the range of wavelengths authorized by the geometry of the system extends from $\lambda_\mu = 25\,\mu m$ to $\lambda_g = 4600\,\mu m$. It is seen that, for the three values of R considered in Table 1, the most probable finger wavelength lies above λ_μ and well below λ_g. Therefore, in these cases, the geometry of the column does not hamper the development of the VF instability.

Several particular situations resulting from the interplay of the constraints of the physics and of the system geometry can be encountered. For large viscosity ratios (large R values), it might happen that λ_m, which is proportional to $1/R$, becomes lower than λ_μ. For the typical system considered in Table 1, this would happen for $R \geq 2.44$, i.e. $\eta_1/\eta_2 \geq 11.5$. In these cases, the physics of the VF phenomenon becomes more complex to investigate, even in the linear regime, since the Darcy law is not applicable at the required scale. Besides, for very narrow columns, no fingering will be observed even in presence of unfavorable viscosity ratios if $\lambda_g < \lambda_c$. As seen in Table 1, for $R = 0.307$, this is the case if $d_c < 82\,\mu m$. This observation explains why Fernandez et al. [42] used a column made of a large number of parallel capillaries which are slurry packed for reducing VF. However, the technological difficulties associated with the identical packing of the capillaries and with the even sample distribution across the capillary assembly limit the application of this column design. The limiting column diameter for which λ_g is equal to λ_c becomes smaller when R increases, but then λ_g becomes closer to λ_μ, as the number of particles per column diameter becomes smaller. When this number becomes smaller than about five, λ_g becomes smaller than λ_μ and the VF phenomenon, if present, cannot be described by the model used in Section 3.1. On the other side, for preparative chromatography, for which d_c, and hence λ_g, is large, λ_m is well smaller than λ_g as long as the viscosity ratio is reasonably large. This explains, on the basis of pure LSA arguments, why VF is of increasing importance in columns of increasing diameter. In the nonlinear regime, the effects of VF last longer if more fingers are present at onset in larger columns, which explains why VF is expected to be of crucial importance in preparative chromatography.

5.3. Comparison with experiments

Although evidence of the occurrence of VF in chromatographic columns is known since the sixties in the SEC mode [11] and since the nineties in the RPLC mode [35], there is no quantitative data over the numbers, wavelengths and growth rates of fingers in the chromatographic literature. In some situations, the appearance of multiple peaks or of bumps on the chromatographic peak profile recorded at the column outlet is the signature of the VF phenomenon. Nevertheless, in some cases, a few visualization studies have demonstrated that VF clearly occurs within the chromatographic column but is not detected on the chromatographic peak profile, although it has contributed to increase the peak width [39,47].

In spite of the absence of quantitative data on the VF characteristics, it is worth to examine the influence of various operating parameters on the VF pattern in the optical visualization experiments of Shalliker and coworkers [45–48] at the light of the theoretical results presented above. These experiments were performed by injecting a sample in a packed glass column filled with a mobile phase, the refractive index of which is equal to that of the packing, hence rendering the column transparent. For better visualization of the VF pattern, the sample has a lower viscosity than the eluent, hence the fingers develop at the leading edge of the sample zone, as very clearly illustrated in the various photographs. It was found on images taken at the same position along the column that the growth of the fingers increases with increasing flow rate (Fig. 3 of [45]). This appears to be in contradiction with the expectation derived in Section 4.2 on the basis of the linearity of the ω_m versus ν curve in Fig. 11. However, the experiments were performed in a very low ν range, from 0.3 to 2, and a close look at Fig. 11 shows that, in this ν range, ω_m increases faster than ν, hence $\omega_m t$, which is proportional to ω_m/u, increases with the flow velocity, in agreement with the observations. In addition, in this comparison, it should be kept in mind that the plate height parameters of the experimental column may not be similar to those used for building Fig. 11.

The influence of the viscosity contrast on the finger characteristics is clearly apparent on the photographs of Fig. 4 of [47]. Experiments were performed at R-values of 0.10, 0.21, 0.37, 0.82 and 1.5. In spite of the fact that some caution is required in interpreting the photographs since they are 2D projections on a photographic plate of a 3D VF pattern and that the dynamics might already be in the nonlinear regime, the length of the fingers and their number increase very clearly with increasing R. This is qualitatively in agreement with the expectations. Indeed, at the onset of VF, the number of fingers in the column cross-section should be proportional to k_m^2, hence to R^2, and their length proportional to $\exp(\omega_m t)$, hence to $\exp(R^2)$. That the finger length increases with time is clearly observed in the photographs of Fig. 5 of [47].

The finger width is reported to be between one-quarter and one-half of the column radius in [45], i.e. between 2.1 and 4.3 mm for the photographs of Fig. 5 of [45] obtained at a R-value of 0.77 for a mean particle size of 21 μm. It is seen from Fig. 10, at a ν value of 1, that k_m should be equal to $0.30R/d_p$, which gives a wavelength of 0.6 mm. This is smaller than the reported value, but still of the same order of magnitude. This discrepancy may come from the fact that the plate height parameters constants A–E in the plate height Eqs. (48) and (49) are quite different from typical ones. Besides, and most likely, the reported finger widths were measured in conditions where the VF pattern is well developed and where the linearity assumptions of the LSA model are no longer fulfilled. It is well known that, when the VF dynamics becomes nonlinear, the dynamics is dominated by coarsening: fingers tend to merge together, which leads to a constant increase of the finger wavelength and a decrease in the total number of fingers [6,55,79]. As the fingers of Fig. 5 of [45] are most likely in the nonlinear regime (coarsening is visible from one plate to another) it is then logical that their wavelength observed on the photograph is larger than the value predicted at

onset. In this perspective, careful experimental measurements of the change of the averaged wavelength of the fingers as a function of time would be most welcome.

5.4. Start of the viscous fingering phenomenon and influence of the noise

The simple model described in Section 2.1 describes how a perturbation on the position of the interface between two fluids can give rise to the VF phenomenon and the LSA provides the growth rate of any initial wavy noise on the step interface between the two fluids. Hence the question arises of what is triggering the initial perturbation or where does the noise come from.

In fact, even if the injection device is able to deliver a perfectly planar initial front, there are concentration fluctuations of the interface arising from the thermodynamic noise, linked to the thermal motions of the molecules. Even if infinitesimal, such a noise, which is always present in the experiments, is amplified provided that its characteristic length scale is larger than the critical one, λ_c. Such a noise is random in nature. Besides, a perturbation can be triggered by any accidental change in ambient conditions, such as, for instance, a slight temperature or pressure change, a mechanical vibration of the table or of the ground, slight fluctuations of the electrical power supply which may perturb the operation of the flow delivery system. All these sources of fluctuations are uncontrolled and occur randomly. The resulting flow fluctuations are therefore irreproducible. This explains why the finger pattern in visualization experiments or the chromatographic peak shapes, when VF occurs, were sometimes lacking reproducibility [33–37,45,48]. In addition, a little perturbation of the interface could clearly come from an irregular packing. In that case, the porous medium is not homogeneous and its permeability becomes a function of space. The influence of spatial variations of permeability on fingering has already been studied analytically and numerically in the past [41,80–83]. Such a situation is clearly more complicated than the situation we want to address here and moreover might lead to think that fingering is driven by heterogeneities while it is driven by viscosity differences. Still, if such heterogeneities are the main source triggering the flow perturbations, the instability is expected to be reproducible, at least, at its onset, since these heterogeneities are present at the same location when experiments are repeated. This might also be the case when VF is occurring with column headers with unperfect frit elements.

5.5. Comparison of the chromatographic and VF time and length scales

The physical models of the viscous fingering instability as well as many other hydrodynamic instabilities describe the onset of the instabilities in terms of dispersion relations, growth rates and wavenumbers (or wavelengths). Still, in the chromatographic context, the amplitude is of crucial importance as it determines the extent of the contribution of the instability to peak broadening and, hence, to the loss of chromatographic resolution.

The LSA provides the initial growth rate of the perturbations. Thus, the question arises of the value of the initial amplitude, ϕ, of the perturbations. In a porous packing, it seems reasonable to scale the value of ϕ for the concentration perturbation of the interface to the particle size, d_p:

$$\phi = \beta d_p \tag{53}$$

where the value of the numerical constant β is expected to be close to 1 [84]. The knowledge of the exact value of β is not crucial. Indeed, as the perturbation grows exponentially, it becomes amplified by a factor 10^3 after a time equal to $7\tau_{VF}$. Therefore, even if the actual value of β is as low as 10^{-3}, it takes a time only $7\tau_{VF}$ longer for the perturbation to reach a certain amplitude than if β is equal to 1. When the VF characteristic time, τ_{VF}, is as short as those values reported in Table 1 (about 50 ms for $R = 1$), such a time delay is insignificant compared to the typical residence time of the sample in the column. For operating conditions selected in Table 1, the hold-up time is 105 or 175 s for a 15 or 25 cm long column, respectively. Nevertheless, the influence of VF on the peak shape may not be perceptible if τ_{VF} is not much smaller than t_o, i.e. for small R-values since τ_{VF} is proportional to $1/R^2$. In conditions of Table 1, τ_{VF}/t_o (for a 15 cm long column) becomes larger than 5% for R smaller than 0.10, i.e. η_1/η_2 smaller than 1.1. A 10% difference in viscosity between sample and eluent was the limit above which a significant loss in efficiency was observed by Cherrak et al. [34]. Besides, this may explain that VF was not (or only little) observed for the lowest R-values in Catchpoole et al. [47] experiments, keeping in mind that their operating conditions were different from those of Table 1. Still, for moderate and large R-values, the perturbations grow very fast and are much likely to influence peak shape and broadening. For instance, for $R = 0.3$ ($\eta_1/\eta_2 = 1.35$), in conditions of Table 1, it takes only 4.6 s for a perturbation to grow from one particle diameter (5 μm) to 1 cm, a length clearly distinguishable in the optical system of Shalliker and coworkers [45–48].

We have noted in Section 3.1 that the LSA, which deals with one interface, can be considered as applicable to chromatography as long as the two interfaces of the sample plug do not interact, i.e. as long as the time is shorter than about $L_{inj}^2/(32D_{ax})$. This time, obviously, depends on the injection volume. In conditions of Table 1, for a typical injection volume of 20 μl, the length of the sample plug within the column is 0.17 cm, and the time of persistence of the injection concentration plateau is equal to 9.7 s. It is therefore not short compared to the above time of growth of the instability. Therefore, in practice, this finite length of the sample plug is not limiting the application of the LSA for a single unstable interface to the chromatographic situation.

5.6. Origin of viscosity contrast in liquid chromatography

In the physical model on which this study is based, the instability at the interface between two fluids, 1 and 2, as shown in Fig. 1, was described in the linear domain. In the discussion, we have considered that this is applicable to the chromatographic

situation where that interface is the unstable interface between the sample and the eluent, i.e. the rear interface if the sample is more viscous than the eluent and the front interface in the opposite case. The concentration c is the mole fraction of fluid 1 in the binary fluid mixture. In practice, the sample is never a pure chemical species, but contains at least two chemical species, the sample solvent and a solute (when chromatography is performed for separation purposes, there are of course several solutes in the sample solvent). Therefore, two limiting situations can be encountered: case (a), the sample solvent is identical to the eluent (they may be pure chemical species or mixtures) and the solute is the source of the increase of the viscosity of the sample; case (b), the sample solvent is different from the eluent and has a viscosity sufficiently different from that of the eluent in order to give rise to the VF phenomenon, the solute being a passive species as far as the viscosity of the sample is concerned. The first situation is that mostly encountered in SEC, the second one being that occurring in RPLC [35–37,48].

The ability of a solute to enhance the viscosity of a solution is reflected through its intrinsic viscosity, $[\eta]$, defined as [85a]:

$$[\eta] = \lim_{c_m \to 0} \frac{(\eta/\eta_o) - 1}{c_m} = \lim_{c_m \to 0} \frac{\ln(\eta/\eta_o)}{c_m} \tag{54}$$

where c_m is the mass concentration of the solute in the solution (in g ml^{-1}), η and η_o the viscosities of the solution and of the pure solvent, respectively. In the situation of case (a), it appears by comparing Eqs. (20) and (54) that, for highly diluted solutions:

$$R = [\eta] c_{m,inj} \tag{55}$$

where $c_{m,inj}$ is the mass concentration of the solute in the injected sample. In the case of solutions of homologous series, such as linear homopolymers, the intrinsic viscosity is related to the molar mass, M, of the solute according to the Mark–Houwink–Sakurada equation:

$$[\eta] = KM^{\alpha} \tag{56}$$

where the constants K and α vary with polymer or homologous series type, solvent and temperature [30b,85b]. The R-value for the solution depends on both the solute molar mass and its concentration in the injected sample. The molar mass, M_{req}, required to reach a certain value of R is then given as:

$$M_{req} = \left(\frac{R}{K c_{m,inj}} \right)^{1/\alpha} \tag{57}$$

For instance, for a typical polymer concentration in the injected sample of 0.001 g/ml, the required molar mass for reaching $R = 0.2$ (and thus $[\eta] = 200$ ml g^{-1}) is calculated to be equal to 7.5×10^5 g mol^{-1} for polystyrene in toluene at 30 °C and to 2.5×10^5 g mol^{-1} for polyethyleneoxide in water at 30 °C [86]. Although the values of the Mark–Houwink–Sakurada parameters of other solute/solvent systems may be quite different from these ones, these calculations illustrate that rather high solute molar masses are required to get a sufficient intrinsic viscosity for observing the VF phenomenon. This is why VF arising with relatively diluted solute/eluent systems has been mainly observed in SEC of high molar mass polymer solutions.

In other LC retention modes, VF is encountered in case (b) situations, when the viscosity contrast arises essentially between the sample solvent and the eluent, the solutes of relatively low molar masses being at a dilution level such that they have no significant influence on the viscosity of the solution. In that case, as far as VF is concerned, the system is again, as above, a binary mixture. However, the relatively low molar mass of the sample solvent, and its associated generally low intrinsic viscosity, is compensated by its rather large mass concentration in the eluent. For instance, $R = 0.2$ is reached for a sample solvent concentration of 0.067 g ml^{-1} for methanol in water or of 0.082 g ml^{-1} for glycerol in water. Then, the influence of the VF perturbations on the solute peak shapes is likely to depend on the retention factor of the solute. Unretained solutes with dispersion characteristics similar to those of the sample solvent will be affected as this solvent by the VF phenomenon. Instead, the bands of highly retained solutes, which are soon disengaged from the sample solvent band as they migrate along the column, are likely to be little perturbed by the VF phenomenon affecting this solvent band. The discussion on the influence of the retention factor on the solute peak shapes, although of primary importance for the significance of the VF phenomenon on the chromatographic separation, is behind the scope of the present study and will be presented in a forthcoming publication.

In the RPLC mode, eluents and sample solvents are frequently water–methanol or water–acetonitrile solutions of various compositions. Such solutions may have a non-monotonic viscosity–concentration profile (whether this profile is monotonic or not depends on the compositions on the eluent and of the sample solvent). Manickham and Homsy [55] have shown that, in the particular case of isotropic dispersion ($\varepsilon = 1$), the dispersion relation for fluids with a non-monotonic viscosity–concentration profile, as well as for monotonic ones which do not follow Eq. (20), is still expressed by Eq. (37) in which R is replaced by the parameter Λ defined as:

$$\Lambda = \frac{\eta_2}{\eta_1 + \eta_2} \left[\left. \frac{d(\eta/\eta_2)}{dc} \right|_{c=0} + \left. \frac{d(\eta/\eta_2)}{dc} \right|_{c=1} \right] \tag{58}$$

It can be verified that, for the particular case where $\eta(c)$ is given by Eq. (20), one has $\Lambda = R$. The above result can be extended to any value of ε. Therefore, the results presented in this study regarding the growth rates, wavenumbers or wavelengths, and time scales, as functions of R at the onset of VF for an unstable step interface can be extended to any eluent-sample mixture by replacing R by Λ in the corresponding expressions.

5.7. Effect of the sample volume

As discussed above (especially in Section 5.5), since the LSA provides informations on the early times of development of the VF instability, it is limited to the description of what happens at that sample-eluent interface where the viscosity contrast is unfavorable and triggers the instability. It can therefore not take into account the influence of the injected sample volume on the VF pattern at the onset of VF. Nevertheless, if during the linear regime of growth of the instability, the fingers growing from one

interface reach the other sample-eluent interface, their growth will not be that of a single interface anymore. An estimate of the limiting time, t_{lim}, at which this would happen if the finger growth was still occurring in the linear regime can be obtained by combining Eqs. (28), (52) and (53):

$$t_{lim} = \frac{1}{\omega_m} \ln\left(\frac{L_{inj}}{\beta d_p}\right) = \tau_{VF} \ln\left(\frac{L_{inj}}{\beta d_p}\right) \quad (59)$$

For a typical injection volume of 20 μl and column characteristics reported in Table 1, taking $\beta = 1$ for the initial amplitude of the perturbation, this limiting time is 5.8 times larger than the characteristic VF time. This time, like τ_{VF}, is proportional to $1/R^2$.

It is, however, likely that, in usual chromatographic conditions, this limiting time exceeds the transition time at which the finger growth ceases to occur in the linear regime for which the LSA is applicable, i.e. at which fingers cease to increase exponentially as time elapses. The computation of this time requires an elaborate treatment which is out of the scope of the present study. Still, the influence of the sample volume has already been illustrated by numerical simulations in the nonlinear regime [79].

6. Conclusion

The phenomenon of viscous fingering occurs as soon as a fluid is displaced by a less viscous one in a porous medium (for fluids with a monotonic viscosity–concentration profile). Such a contrast of viscosity is most generally present between the carrier liquid and the sample in a liquid chromatographic system. This VF phenomenon leads to peak shape distortion and band broadening as has been observed on recorded peak shapes at the column outlet or by various methods of in-column visualization. Still, the detrimental influence of this phenomenon on the separation performances is rarely considered when selecting the operational conditions for separations.

The linear stability analysis of this phenomenon at its onset shows that the interface is unstable as soon as R (or Λ) >0. It provides informations on the most probable values of the rate of growth of the perturbations and on their wavenumbers (i.e. on their extension in a direction transverse to that of the flow) when the phenomenon starts, i.e. when they are the largest. In practice, these quantities can easily be computed by means of the single curves for ω_m and k_m in Figs. 10 and 11, for any combination of the carrier velocity, the particle size, the solute diffusion coefficient and the sample/eluent viscosity ratio. On the basis of the typical values of the operating parameters encountered in analytical LC, we have shown that, for a R-value of 0.2 (i.e. a viscosity difference of only 22% between sample and eluent), a perturbation of the size of one particle should reach an amplitude of 1 cm in about 7 s which is well shorter than the typical hold-up time. This illustrates that the contribution of VF to the deterioration of the performances cannot be ignored.

Therefore, quantitative experimental studies of VF in chromatography would be welcome. By measuring the time dependence of the fingers wavelength and of the logarithm of the amplitude of the fingers, they would allow to investigate the growth rate and most unstable wavenumber characterizing the onset of the VF instability. Beyond this linear regime, a measure of these quantities on longer time scales would allow to follow the transition from the linear regime, where the LSA is applicable, to the nonlinear regime where fingers are sufficiently developed to interact together. Simulations of this nonlinear regime in chromatographic conditions will be presented in a forthcoming publication.

Nomenclature

A	constant of the axial plate height equation (Eq. (48))
A_p	initial amplitude of the perturbation
B	constant of the axial plate height equation (Eq. (48))
c	concentration (mole fraction) of the downstream, more viscous fluid in the binary fluid mixture
c_m	mass concentration of the solute in the solution (in g/ml)
$c_{m,inj}$	mass concentration of the solute in the injected sample
C	constant of the axial plate height equation (Eq. (48))
d_p	particle size
D	constant of the transverse plate height equation (Eq. (49))
D_{ax}	axial dispersion coefficient
D_{tr}	transverse dispersion coefficient
E	constant of the transverse plate height equation (Eq. (49))
g	gravitational acceleration
h_{ax}	reduced axial plate height
H_{ax}	axial plate height
h_{tr}	reduced transverse plate height
H_{tr}	transverse plate height
k	wavenumber defined by Eq. (30)
K	constant of the Mark–Houwink Eq. (55)
k_c	critical (or cut-off) wavenumber
k_g	geometrical low-value cut-off wavenumber imposed by the column diameter
k_m	most probable (or most dangerous) wavenumber
k_p	column permeability
k_x, k_y	wavenumbers in the x and y directions, respectively
k_μ	cut-off wavenumber arising from the microscopic scale of the porous medium
L_c	column length
L_{inj}	length occupied by the sample plug in the column just after injection
L_{ref}	reference length defined by Eq. (30)
P	pressure
P_{in}	inlet pressure
P_{out}	outlet pressure
P_z	pressure at position z
Q	flow rate
R	logmobility ratio defined by Eq. (22)
t	time
t_{lim}	limiting time of growth of the instabilities in the linear regime, expressed by Eq. (59)
t_o	column hold-up time

t_{ref} reference time defined by Eq. (31)
u_A flow velocity in section A
u_B flow velocity in section B
u_c critical velocity (Eq. (10))
x, y transverse directions perpendicular to the flow direction
z position along the column or the porous medium; flow direction

Greek symbols
α constant of the Mark–Houwink–Sakurada Eq. (55)
β numerical constant in Eq. (53)
δ flow orientation indicator
δz length of the perturbation
ΔP pressure drop along the column
ΔP_{app} applied pressure drop
ΔP_{stat} hydrostatic pressure
$\Delta\eta$ viscosity difference
$\Delta\rho$ density difference
ε dispersion ratio defined by Eq. (36)
ε_{tot} total porosity of the column
η fluid viscosity
η_1 viscosity of fluid 1
η_2 viscosity of fluid 2
η_o viscosity of the pure solvent
$[\eta]$ intrinsic viscosity of a solute, defined by Eq. (54) (in ml g^{-1})
Λ generalized viscosity parameter for any viscosity–concentration profile, defined by Eq. (58)
λ_c critical (or cut-off) wavelength
λ_g geometrical high-value cut-off wavelength imposed by the column diameter
λ_m most probable (or most dangerous) wavelength
λ_μ low-value cut-off wavelength arising from the microscopic scale of the porous medium
ν reduced velocity
ρ fluid density
ρ_1 density of fluid 1
ρ_2 density of fluid 2
τ_{VF} characteristic onset time of the VF pattern
ϕ initial amplitude of a perturbation
Φ amplitude of a perturbation
ω growth rate of the instability
ω_m maximum growth rate of the instability

Subscript
o base state parameters (in absence of instabilities)

Superscript
$*$ dimensionless quantities

Acknowledgements

A.D.W. and M.M. warmly thank G.M. Homsy for introducing them to the physics of viscous fingering and for enlightening discussions. This work was supported by the French-Belgian governmental program, Tournesol 2005–2006 (Programme d'Actions Intégrées n° 08948YD). GR and ADW have benefited from the financial support of the Francqui Foundation. ADW acknowledges also grants from FNRS and from the Communauté française de Belgique under the "Actions de Recherches Concertées" Programme. GR and ADW would like to thank ISRIB (Institute for the encouragement of Scientific Research and Innovation of Brussels) for financial support.

References

[1] C.T. Tan, G.M. Homsy, Phys. Fluids 29 (1986) 3549.
[2] J.C. Giddings, Unified Separation Science, Wiley-Interscience, New York, 1991, p. 141.
[3] U.D. Neue, D.H. Marchand, L.R. Snyder, J. Chromatogr. A 1111 (2006) 32.
[4] S. Hill, Chem. Eng. Sci. 1 (1952) 247.
[5] P.G. Saffman, G. Taylor, Proc. R. Soc. Lond. Ser. A 245 (1958) 312.
[6] G.M. Homsy, Ann. Rev. Fluid Mech. 19 (1987) 271.
[7] H.S. Hele-Shaw, Trans. Inst. Naval Architects, Lond. 40 (1898) 21.
[8] In passing it is interesting to note that many field-flow fractionation channels in use today are nothing else than Hele–Shaw cells.
[9] (a) J. Bear, Dynamics of Fluids in Porous Media, American Elsevier, New York, 1972 (Dover, New York, 1988), p. 687;
(b) J. Bear, Dynamics of Fluids in Porous Media, American Elsevier, New York, 1972 (Dover, New York, 1988), p. 544;
(c) J. Bear, Dynamics of Fluids in Porous Media, American Elsevier, New York, 1972 (Dover, New York, 1988), p. 19.
[10] P. Flodin, J. Chromatogr. 5 (1961) 103.
[11] K.H. Altgelt, J.C. Moore, in: M.J.R. Cantow (Ed.), Polymer Fractionation, Academic Press, New York, 1967, p. 164.
[12] R.E. Collins, Flow of Fluids through Porous Materials, Reinhold Publ. Co., New York, 1961, p. 196.
[13] J.C. Moore, Sep. Sci. 5 (1970) 723.
[14] K.P. Goetze, R.S. Porter, J.F. Johnson, J. Polym. Sci., Part A-2 9 (1971) 2255.
[15] J.H. Duerken, A.E. Hamielec, J. Appl. Polym. Sci. 12 (1968) 2225.
[16] J.N. Little, J.L. Waters, K.J. Bombaugh, W.J. Pauplis, J. Polym. Sci., Part A-2 7 (1969) 1775.
[17] J.N. Little, J.L. Waters, K.J. Bombaugh, W. Pauplis, J. Chromatogr. Sci. 9 (1971) 341.
[18] A. Rudin, J. Polym. Sci., Part A-1 9 (1971) 2587.
[19] K.H. Altgelt, in: J.C. Giddings, R.A. Keller (Eds.), Advances in Chromatography, vol. 7, Dekker, New York, 1968, p. 3.
[20] K.A. Boni, F.A. Sliemers, P.B. Stickney, J. Polym. Sci. Part A-2 (1968) 1567.
[21] A. Lambert, Polymer 10 (1969) 213.
[22] W.W. Yau, C.P. Malone, H.L. Suchan, Sep. Sci. 5 (1970) 259.
[23] J. Janča, J. Chromatogr. 134 (1977) 263.
[24] J. Janča, S. Pokorný, J. Chromatogr. 148 (1978) 31.
[25] J. Janča, S. Pokorný, J. Chromatogr. 170 (1979) 319.
[26] J. Janča, S. Pokorný, L.Z. Vilenchik, B.G. Belenkii, J. Chromatogr. 211 (1981) 39.
[27] S. Yamamoto, M. Nomura, Y. Sano, J. Chem. Eng. Jpn. 19 (1986) 227.
[28] J. Janča, J. Chromatogr. 170 (1979) 309.
[29] O. Chiantore, M. Guaita, J. Chromatogr. 353 (1986) 285.
[30] (a) W.W. Yau, J.J. Kirkland, D.D. Bly, Modern Size-Exclusion Liquid Chromatography, Wiley, New York, 1979, p. 243;
(b) W.W. Yau, J.J. Kirkland, D.D. Bly, Modern Size-Exclusion Liquid Chromatography, Wiley, New York, 1979, p. 291.
[31] L.R. Snyder, J.J. Kirkland, Introduction to Modern Liquid Chromatography, second ed., Wiley, New York, 1979, p. 507.
[32] C.H. Byers, W.G. Sisson, J.P. DeCarli II, G. Carta, Biotechnol. Prog. 6 (1990) 13.
[33] M. Czok, A.M. Katti, G. Guiochon, J. Chromatogr. 550 (1991) 705.
[34] D. Cherrak, E. Guernet, P. Cardot, C. Herrenknecht, M. Czok, Chromatographia 46 (1997) 647.

[35] R.C. Castells, C.B. Castells, M.A. Castillo, J. Chromatogr. A 775 (1997) 73.
[36] C.B. Castells, R.C. Castells, J. Chromatogr. A 805 (1998) 55.
[37] S. Keunchkarian, M. Reta, L. Romero, C. Castells, J. Chromatogr. A 1119 (2006) 20.
[38] K.H. Altgelt, Sep. Sci. 5 (1970) 777.
[39] L.D. Plante, P.M. Romano, E.J. Fernandez, Chem. Eng. Sci. 49 (1994) 2229.
[40] E.N. Lightfoot, A.M. Athalye, J.L. Coffman, D.K. Roper, T.W. Root, J. Chromatogr. A 707 (1995) 45.
[41] E.J. Fernandez, C.A. Grotegut, G.W. Braun, K.J. Kirschner, J.R. Staudaher, M.L. Dickson, V.L. Fernandez, Phys. Fluids 7 (1995) 468.
[42] E.J. Fernandez, T.T. Norton, W.C. Jung, J.G. Tsavalas, Biotechnol. Prog. 12 (1996) 480.
[43] Q.S. Quan, A. Rosenfeld, T.W. Root, D.J. Klingenberg, E.N. Lightfoot, J. Chromatogr. A 831 (1999) 149.
[44] M.L. Dickson, T.T. Norton, E.J. Fernandez, AIChE J. 42 (1997) 409.
[45] B.S. Broyles, R.A. Shalliker, D.E. Cherrak, G. Guiochon, J. Chromatogr. A 822 (1998) 173.
[46] R.A. Shalliker, B.S. Broyles, G. Guiochon, J. Chromatogr. A 865 (1999) 73.
[47] H.J. Catchpoole, R.A. Shalliker, G.R. Dennis, G. Guiochon, J. Chromatogr. A 1117 (2006) 137.
[48] K.J. Mayfield, R.A. Shalliker, H.J. Catchpoole, A.P. Sweeney, V. Wong, G. Guiochon, J. Chromatogr. A 1080 (2005) 124.
[49] T.T. Norton, E.J. Fernandez, Ind. Eng. Chem. Res. 35 (1996) 2460.
[50] R.B. Bird, W.E. Stewart, E.N. Lightfoot, Transport Phenomena, Wiley, New York, 1960, p. 150.
[51] P. Jacquard, P. Séguier, J. Mécaniq. 1 (1962) 367.
[52] G.M. Homsy, in: E. Guyon, J.-P. Nadal, Y. Pomeau (Eds.), Disorder and Mixing, NATO ASI Series, vol. E152, Kluwer Academic Publishers, Dordrecht, 1988, p. 237.
[53] A.E. Scheidegger, The Physics of Flow through Porous Media, third ed., University of Toronto Press, Toronto, 1974, pp. 229.
[54] J.-C. Bacri, D. Salin, Y.C. Yortsos, C.R. Acad. Sci. Paris, Sér. II 314 (1992) 139.
[55] O. Manickham, G.M. Homsy, Phys. Fluids A 5 (1993) 1356.
[56] C.C. Lin, The Theory of Hydrodynamic Stability, Cambridge University Press, 1955, p. 1.
[57] S. Chandrasekhar, Hydrodynamic and Hydromagnetic Stability, Dover, New York, 1981, p. 1.
[58] (a) G. Guiochon, A. Felinger, D.G. Shirazi, A.M. Katti, Fundamentals of Preparative and Nonlinear Chromatography, second ed., Elsevier, Amsterdam, 2006, p. 60;
(b) G. Guiochon, A. Felinger, D.G. Shirazi, A.M. Katti, Fundamentals of Preparative and Nonlinear Chromatography, second ed., Elsevier, Amsterdam, 2006, p. 262;
(c) G. Guiochon, A. Felinger, D.G. Shirazi, A.M. Katti, Fundamentals of Preparative and Nonlinear Chromatography, seconded., Elsevier, Amsterdam, 2006, p. 310.
[59] L. Lebon, J. Leblond, J.-P. Hulin, Phys. Fluids 9 (1997) 481.
[60] B.E. Poling, J.M. Prausnitz, J.P. O'Connell, The Properties of Gases and Liquids, fifth ed., McGraw-Hill, Boston, 2001, p. 9.77.
[61] S. Arrhenius, Zeitschr. physikal. Chem. 1 (1887) 285.
[62] S. Arrhenius, Biochem. J. 11 (1917) 112.
[63] J. Crank, The Mathematics of Diffusion, second ed., Clarendon Press, Oxford, 1975, p. 215.
[64] F.S. Crawford Jr., Waves, Berkeley Physics Course, vol. 3, Education Development Center, Newton, 1968 (French Edition, Armand Colin, Paris, 1972), p. 58.
[65] R.L. Chouke, unpublished work, reported in appendix of J.W. Gardner, J.G.J. Ypma, Soc. Petrol. Eng. J. 24 (1984) 508.
[66] J.C. Giddings, Anal. Chem. 35 (1963) 1338.
[67] E. Grushka, L.R. Snyder, J.H. Knox, J. Chromatogr. Sci. 13 (1975) 25.
[68] S.G. Weber, P.W. Carr, in: P.R. Brown, R.A. Hartwick (Eds.), High Performance Liquid Chromatography, Wiley, New York, 1989, p. 1.
[69] T.K. Perkins, O.C. Johnston, Soc. Petrol. Eng. J. 3 (1963) 70.
[70] J.M.P.Q. Delgado, Heat Mass Transfer 42 (2006) 279.
[71] A.J.P. Martin, R.L.M. Synge, Biochem. J. 35 (1941) 1358.
[72] J.C. Giddings, Nature 184 (1959) 357.
[73] J.N. Done, G.J. Kennedy, J.H. Knox, in: S.G. Perry (Ed.), Gas Chromatography 1972, Applied Science Publ., Barking, UK, 1973, p. 145.
[74] J.H. Knox, G.R. Laird, P.A. Raven, J. Chromatogr. 122 (1976) 129.
[75] C. Eon, J. Chromatogr. 149 (1978) 29.
[76] U. Tallarek, E. Bayer, G. Guiochon, J. Am. Chem. Soc. 120 (1998) 1494.
[77] Y.C. Yortsos, M. Zeybek, Phys. Fluids 31 (1988) 3511.
[78] W.B. Zimmerman, G.M. Homsy, Phys. Fluids A 4 (1992) 2348.
[79] A. De Wit, Y. Bertho, M. Martin, Phys. Fluids 17 (2005) 054114.
[80] C.T. Tan, G.M. Homsy, Phys. Fluids A 4 (1992) 1099.
[81] H.A. Tchelepi, F.M. Orr Jr., N. Rakotomalala, D. Salin, R. Wouméni, Phys. Fluids A 5 (1993) 1558.
[82] (a) A. De Wit, G.M. Homsy, J. Chem. Phys. 107 (1997) 9609;
(b) A. De Wit, G.M. Homsy, J. Chem. Phys. 107 (1997) 9619.
[83] C.-Y. Chen, E. Meiburg, J. Fluid Mech. 371 (1998) 269.
[84] C. Chevalier, Ph.D. thesis, Université Pierre et Marie Curie, Paris 6, December 2006.
[85] (a) C. Tanford, Physical Chemistry of Macromolecules, Wiley, New York, 1961, p. 390;
(b) C. Tanford, Physical Chemistry of Macromolecules, Wiley, New York, 1961, p. 407.
[86] M. Kurata, Y. Tsunashima, M. Iwama, K. Kamada, in: J. Brandup, E.H. Immergut (Eds.), Polymer Handbook, second ed., Wiley, New York, 1975, p. IV-18.23.